Bollettino di Geofisica Teorica ed Applicata Vol. 61, n. 4, pp. 375-402; December 2020
DOI 10.4430/bgta0318

Upper mantle discontinuities: anisotropic view on the lithosphere - asthenosphere system

J. Plomerová

Institute of Geophysics, Czech Academy of Sciences, Prague, Czech Republic

(Received: 11 March 2019; accepted: 16 January 2020)

ABSTRACT This paper stems from a keynote "Inge Lehmann Lecture" during the ESC 2018 General Assembly and presents an overview of the historical development of Earth stratification and the corresponding discontinuities to a broader seismological community. The paper concentrates on the role of seismic velocity anisotropy in modelling the lithosphere-asthenosphere system and presents models of the lithosphere-asthenosphere boundary (LAB), the most significant tectonic boundary from the point of view of plate tectonics. With the use of anisotropic characteristics retrieved from both the surface and body waves, we model the LAB discontinuity as a narrow transition between fossil anisotropy within the mantle lithosphere and present-day flow-related anisotropy in the asthenosphere in different tectonic settings within continental and oceanic plates. The lower plate boundary lies in a relatively broad depth interval, from about 50 km beneath Phanerozoic basins up to about 220 km beneath Precambrian cratons and platforms. Beneath the oceanic plates, the discontinuity shallows up to ~30 km or even less. Distinct LAB depth variations at short distances occur particularly in Phanerozoic parts of continents.

Key words: Earth mantle discontinuities, lithosphere-asthenosphere boundary, fossil vs. present-day related large-scale anisotropy.

1. Introduction

In ancient time, people believed the Earth is flat and imagined it as a plane or a disk. In that archaic concept, the Earth was surrounded with a solid sphere, standing on three elephants which stood on a giant turtle. This early vision of the Earth survived until the 6th century B.C., when the Greek philosopher Pythagoras initiated the new concept of the spherical Earth. The spherical shape of the Earth was endorsed around 330 B.C. by Aristotle (e.g. by observing rounded shape of Earth shadow during lunar eclipse) and from then the knowledge of the spherical Earth gradually began to spread beyond the Hellenistic world. The very historical views on the Earth, especially in the beginning, concerned its overall shape, with nothing said about its interior, although the spherical Earth in the Aristotle's view consisted of five elemental spheres: Earth, Water, Wind, Fire and *Primum mobile*. Since then, our knowledge of the Earth shape and its structure has significantly changed, sometimes including very exotic images of the Earth inner structure [e.g. Edmund Halley's "Hollow Earth" theory, Halley (1692)].

In modern times, the interior of the spherical Earth is divided into three basic parts: the crust,

the mantle, and the core. Boundaries between the individual zones within the radial Earth, which differ substantially in their composition, physical parameters (density, temperature, pressure, viscosity, etc.) and particularly in velocities of seismic waves, are considered as discontinuities. The crust-mantle boundary zone, characterised by positive velocity impedance, is called the Mohorovicic (Moho) discontinuity, discovered in 1909 by Andrija Mohorovičić, a Croatian seismologist. Across the core-mantle boundary (CMB), velocities of longitudinal waves decrease significantly and drop to zero for shear waves due to the liquid nature of the core (Fig. 1).

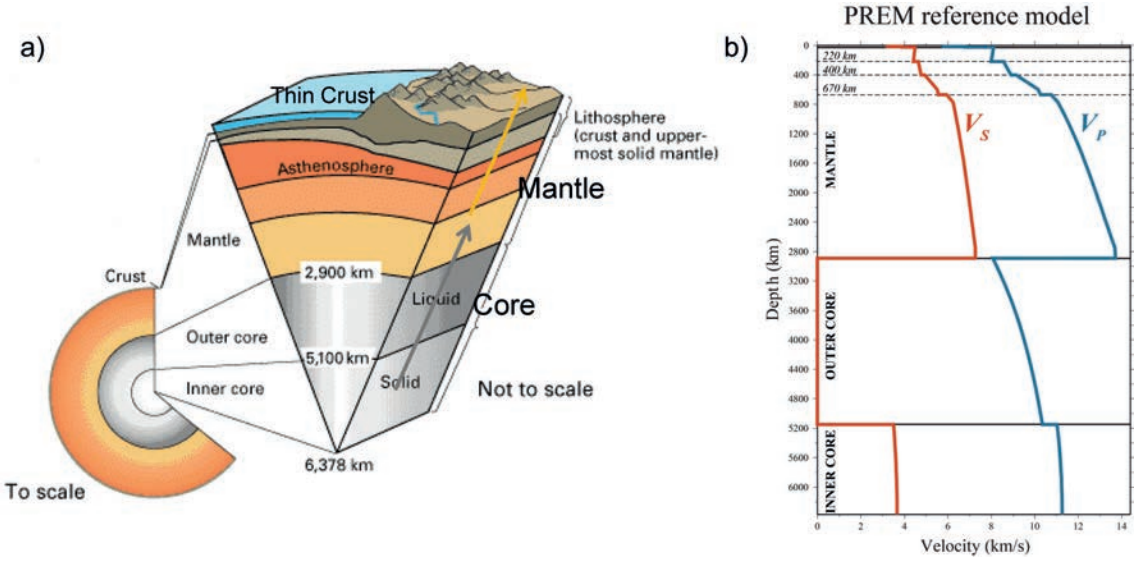

Fig. 1 - a) Internal division of the spherical Earth; b) seismic velocities within the Earth in the PREM model of Dziewonski and Anderson (1981).

The basic division of the Earth interior became more and more complex with increasing number of observations in various geophysical fields. Inge Lehmann discovered in 1936 that the liquid core contains inside a smaller solid core (Lehmann, 1936). Lately, compelling evidence has revealed a seismic velocity discontinuity along N-S paths about 200 km below the inner core boundary separating an isotropic upper inner core from an anisotropic lower inner core (Song and Helmberger, 1998). On the other hand, a number of undisputable discontinuities have been discovered in the mantle by different methods, e.g. from reverberations of shear waves reflected at the Earth interfaces (Revenaugh and Jordan, 1991) (Fig. 2), both at global and regional [e.g. the X discontinuity, see Chen *et al*. (2017) for review] scales. The most distinctive discontinuities at 410 and 660 km, distributed globally over the Earth, relate to mineral phase transitions and frame the Transition Zone (TZ) separating the upper and lower mantle. With the exception of the Gutenberg discontinuity (G) recognized beneath the oceans (Gutenberg, 1959), all the other upper mantle discontinuities exhibit positive impedance *(VQ)* increase, including the Hales (1969) and the Lehmann (1959, 1961) discontinuities in the upper mantle, as well as the 520 km discontinuity within the TZ (Shearer, 1990). The often mentioned Lehmann discontinuity occurs beneath continents at largely variable depth (Anderson, 1979) being ~210 km on average (Fig. 3,

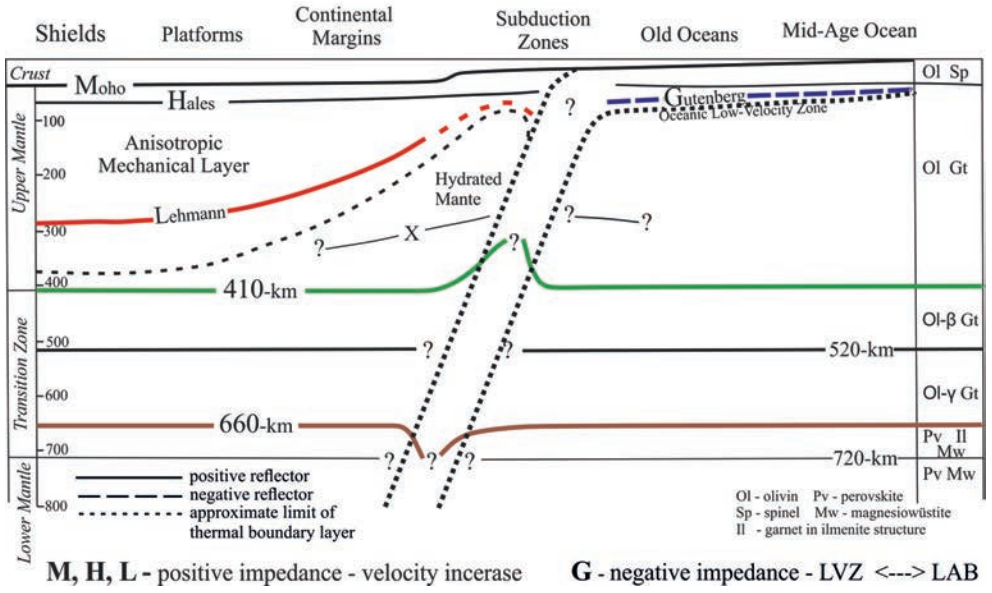

Fig. 2 - Upper mantle discontinuities derived from ScS wave reverberation (redrawn from Revenaugh and Jordan, 1991).

see also Fig. 2), but in some regions, e.g. in central Europe, it is detected only sporadically (Kind *et al*., 2017). Interpretations of this discontinuity are very broad and change with time, but they mostly relate to changes of anisotropy (e.g. Gaherty and Jordan, 1995). Due to a velocity increase across this boundary, it is sometimes related to the bottom of the asthenosphere (Dziewonski and Anderson, 1981), and rarely also to the lithosphere - asthenosphere boundary (LAB) (Gung *et al*., 2003). Direct association of the Lehmann discontinuity with LAB is ruled out due to the velocity increase across this discontinuity.

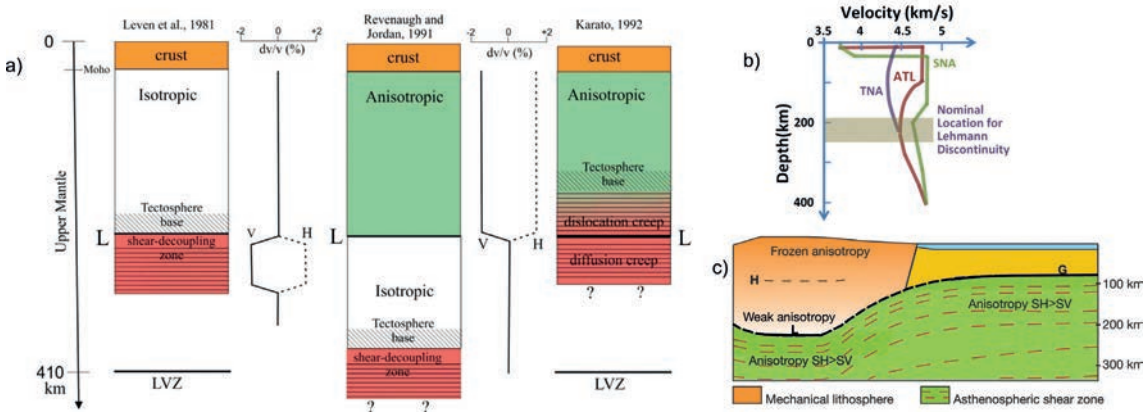

Fig. 3 - a) Hypothesis relating the Lehmann (L) and Gutenberg (G) discontinuities to upper mantle anisotropy (redrawn from Gaherty and Jordan, 1995 and Gung *et al*., 2003); b) shear-velocity changes across the Lehmann discontinuity at tectonically different regions: TNA - tectonic provinces of North America, SNA - shield area of North America, ATL - North Atlantic (after Grand and Helmberger, 1984; Anderson, 2007); c) interpretation of the observed anisotropy in relation to the Lehmann (L), Gutenberg (G) and the Hales (H) discontinuities, after Gung *et al*. (2003).

The need of better understanding the upper mantle discontinuities has increased since the early 20th century, when Alfred Wegener introduced the continental drift hypothesis (Wegener, 1915), a predecessor of the plate tectonic concept. The concept was further developed mainly in the 1960s by Hess (1964), who first coined the term "sea floor spreading". In this idea, the lithospheric plates consisting in the crust and the rigid part of the upper mantle slowly drifts above the viscous asthenosphere. Answering questions concerning the definition of the lithospheric plates and particularly physically delimiting the lower boundary of the plates - the LAB (e.g. Fischer *et al*., 2010) or the internal lithosphere discontinuities [e.g. mid-lithospheric discontinuity (MLD): e.g. Savage and Silver (2008), Hopper and Fischer (2015), Aulbach *et al*. (2017), and Selway (2019)] - became an essential task in last decades (e.g. Cooper *et al*., 2017; Karato and Park, 2019). The LAB represents the first-order structural discontinuity/transition of the Earth interior that accommodates differential motion between the plates and the underlying mantle in the contest of plate tectonics. Although the LAB is the most extensive type of plate boundary on the planet, its definitive detection, especially beneath cratons, remains elusive (Eaton *et al*., 2009). We are used to calling the boundaries within the layered Earth "discontinuities", even though in reality they represent narrow transition zones of different thickness with steep gradients of gradually changing various physical parameters, e.g. seismic wave velocity, mineral composition, electric conductivity, etc.

This contribution is dedicated to the seismological community and aims to give an overview of the historical evolution of the knowledge concerning the stratification of the Earth and the discontinuities; specifically the LAB and MLD, both in continental and oceanic settings, in the recently published monograph are described in details on lithospheric discontinuities by Yuan and Romanowicz (2019).

2. Definitions of the lower plate boundary (LAB)

There are different definitions of the lithosphere and the LAB depending on the physical parameters and methods used. Gutenberg (1959) defined the lithosphere as the high-velocity outer layer of the Earth, underlain by a low-velocity zone, or, a region where the positive velocity gradient decreases. In addition to this original definition of LAB, there are several other fundamental definitions of the lithosphere and its lower boundary (Fig. 4), e.g. mechanical, rheological, compositional, thermal, electrical, petrological, etc. The LAB is a mechanical boundary layer that moves coherently with the plate. The mechanical definition can be understood as a response of the Earth's outer shell to surface loading. This concept assumes a mechanically-strong lithosphere (supporting deviatoric stress over geologically-long periods) overlying a mechanically-weak asthenosphere (allowing a mass flow associated with isostatic adjustment). Rheologically, the LAB lies at depth where shear strength drops below a particular value (e.g. 1 MPa). In the broadly used thermal definition, the LAB is set as a thermal boundary layer between the conductive lid (lithosphere) and adiabatic convective sub-lithospheric mantle, usually associated with 1250°C isotherm (e.g. Priestley *et al*., 2019). The electric definition of the lithosphere, as an electrically-resistive layer above a layer of decreased resistivity, exhibits, similarly to the thermal definition, both horizontally and vertically low resolution (e.g. Praus *et al*., 1990; Korja, 2007). The melt-depleted part of the upper mantle, including deep portions occupied dominantly by melt-

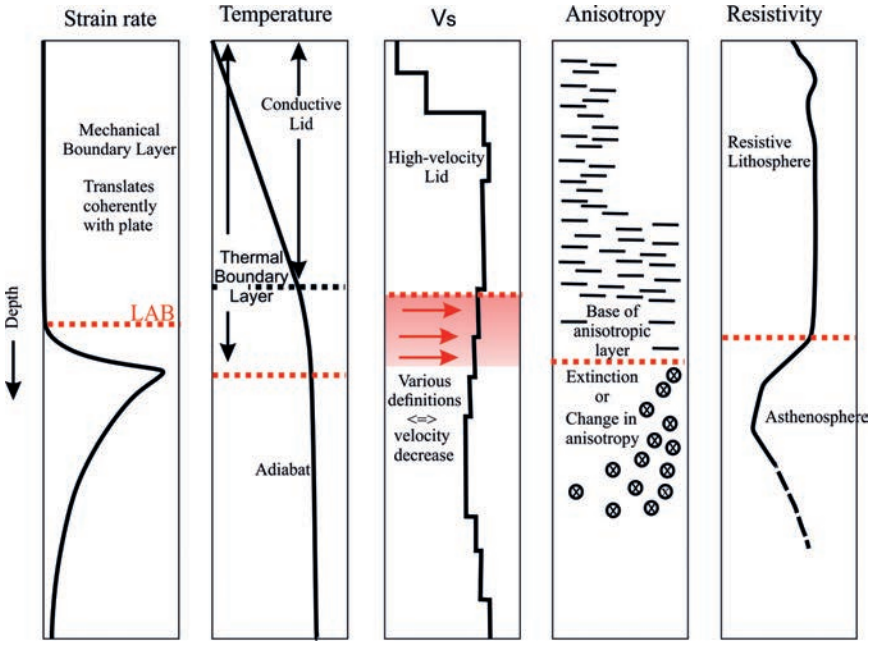

Fig. 4 - Examples of how different disciplines define the lithosphere-asthenosphere boundary (LAB), after Eaton *et al.* (2009).

metasomatised mantle rocks, is considered as the petrologic lithosphere. The most recent study (Karato and Park, 2019) searches for models that would best explain the sharp and large velocity drop across the LAB (MLD), which occurs at relatively too low temperatures to be attributed to partial melting. The authors evaluate the pros and cons of three models characterised as layered anisotropy, layered composition (e.g. Caló *et al.*, 2016) and elastically-accommodated grain-boundary sliding (see also Jackson and Faul, 2010; Olugboji *et al.*, 2013; Karato *et al.*, 2015), and cite the last one as the most probable.

In models with layered anisotropy (Fig. 4), the LAB is associated with a boundary between two layers with differently oriented azimuthal anisotropy, or, between layers whose strengths of anisotropy differ substantially (Eaton *et al.*, 2009 for review). Several independent studies of seismic wave propagation have demonstrated that the large-scale seismic anisotropy reflecting the lattice preferred orientation (LPO) of peridotites, the main constituent of the upper mantle, is a generally spread unchallenged characteristic of the upper mantle (Babuška and Cara, 1991; Ben Ismail and Mainprice, 1998). Azimuthal anisotropy is a powerful tool to study layering structure of the Earth mantle, particularly when combining independent types of data and applying Bayesian inversion approach (Bodin *et al.*, 2016). However, the complex structure of the continental lithosphere (e.g. Plomerová and Babuška, 2010), as revealed from joint inversion/interpretation of body wave anisotropic parameters evaluated in 3D in tectonically different provinces, clearly shows that layered models considering only azimuthal anisotropy do not reflect the structural complexity of the plates. The lithosphere models extending the space degree up to 3, and thus considering models with inclined symmetry axes generally oriented in 3D, broaden the seismic-anisotropy potential to elucidate the LAB discontinuity/transition between the plates and the sub-lithospheric mantle.

In the following sections we will advocate seismic anisotropy as a powerful tool in the complex LAB modelling with the use of different techniques, both at the global and regional scales.

3. Anisotropic models of the LAB

Various definitions of the LAB lead to various estimates of lithosphere thickness, i.e. depth to the LAB. Disagreements among the models might reflect either real differences in the physical fundamentals of various LABs, or inaccuracy and limitations of individual methods. When evaluating different models, one has to keep in mind that even in cases where a strong negative velocity gradient appears beneath the lithospheric lid, an uncertainty of several tens of kilometres in the position of the LAB should be noted (Eaton *et al*., 2009).

3.1. LAB models from surface wave anisotropy

Proxies of LAB in global models of shear velocities (V_S) derived from surface waves focus on velocity drops or relative deviation from reference models, in general, and relate the shear velocities, temperature, attenuations, and viscosity in the upper mantle (Priestley and McKenzie, 2013). The LAB is set to the depth range of the strongest negative velocity gradient at the base of the high-velocity mantle lid (e.g. Debayle and Kennett, 2000; Priestley and Debayle, 2003) or the depth corresponding to the centre of this gradient (Weeraratne *et al*., 2003). Cotte *et al*. (2002) and Pedersen *et al*. (2013) performed statistical analyses of negative velocity gradients in multiple 1D models to estimate the LAB. For example, Frederiksen *et al*. (2001), Simons and van der Hilst (2002), Gung *et al*. (2003) or Darbyshire *et al*. (2007) take a 1-2% positive velocity anomaly above a global reference model as the LAB depth, whereas Li and Burke (2006) take a specific absolute V_S value instead of a percent velocity anomaly as the LAB proxy. Bruneton *et al*. (2004) applied an array view on changes in the nature of the lateral velocity heterogeneity in a shield region.

However, all the approaches to model the LAB mentioned above tackle the target from the isotropic wave-propagation view, capitalising on significant depth sensitivity of the broad-band (BB) surface waves, though suffering with strong lateral path-integrated effects, i.e. having limited resolution at greater depth (long-period waves). Nevertheless, many surface wave studies model also radial and azimuthal anisotropy within the Earth (e.g. Montagner and Tanimoto, 1991; Ferreira *et al*., 2010; Debayle and Ricard, 2013; Becker *et al*., 2014; Auer *et al*., 2015).

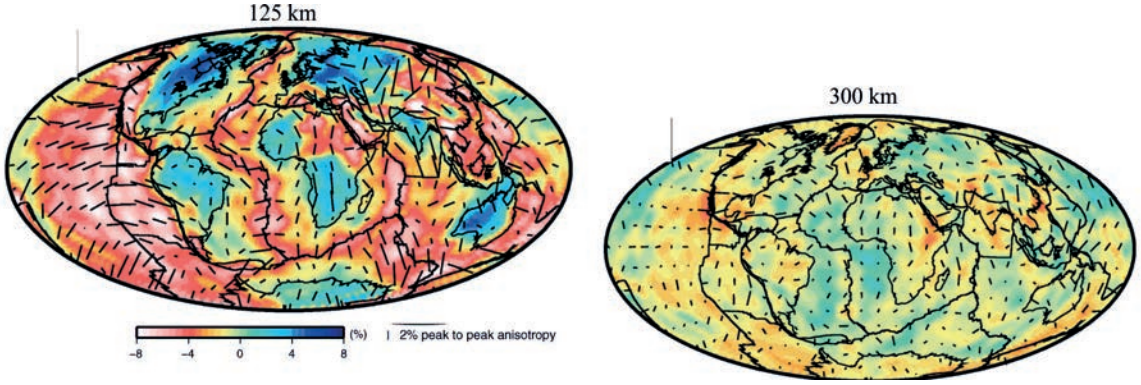

Fig. 5 - Perturbation of V_{Sv} velocities with respect to the pseudo-PREM reference model showing large positive perturbations in the continental lithosphere at 125 km depth against negative perturbations beneath the oceans. All the perturbations decrease significantly with depth (shown for depth of 300 km). The amplitude and orientation of the vectors indicate the fast axis of the azimuthal anisotropy G (after Burgos *et al*., 2014).

The models show rapid decreasing of both the radial ($\xi \sim V_{Sv}/V_{Sh}$) and azimuthal anisotropy G (strength |G|, azimuth ϕ) as one can see in Fig. 5 showing an example of two layers from model of Burgos *et al*. (2014). Correlation between the negative V_{Sv} perturbations calculated with respect to the pseudo-PREM (Preliminary Reference Earth Model) reference model and oceans on one hand, and that between the positive perturbations and continents, with maxima related to cratonic regions on the other, demonstrates the distinct relation between the velocities and their anisotropy with the structure of the plates and the sub-lithospheric mantle. Also Beghein *et al*. (2014) explain the nature of the G discontinuity beneath the oceans by changes in seismic anisotropy.

Plomerová *et al*. (2002b) analysed regional variations of depth dependences of both the radial and azimuthal anisotropy in the upper mantle model by Montagner and Tanimoto (1991). The systematic depth variations of radial anisotropy, could be easily clustered into three main groups related to the Precambrian, the Phanerozoic continental, and the Phanerozoic oceanic provinces. There are also small groups of transitional dependences that reflect a bias in data created when waves pass through two different structures around a grid sample of the region (Fig. 6). We associate the Precambrian mantle characteristics of the radial anisotropy relative to about 2% model anisotropy in the upper 200 km (Montagner and Anderson, 1989), with values below zero. In some locations the radial anisotropy attains even negative absolute values. This implies the world-wide extent of the Precambrian mantle lithosphere is larger than that of the Precambrian units in the crust and that the models with $V_{Sh} > V_{Sv}$ is not valid generally, but it is rather limited to the oceanic regions. There is no doubt that the surface waves passing through the upper mantle detect two main anisotropic signals, one originating in the lithosphere and the other in the sub-lithospheric mantle. Moreover, characteristics of the anisotropic signal coming from the continental lithosphere clearly relate to its age (Babuška *et al*., 1998).

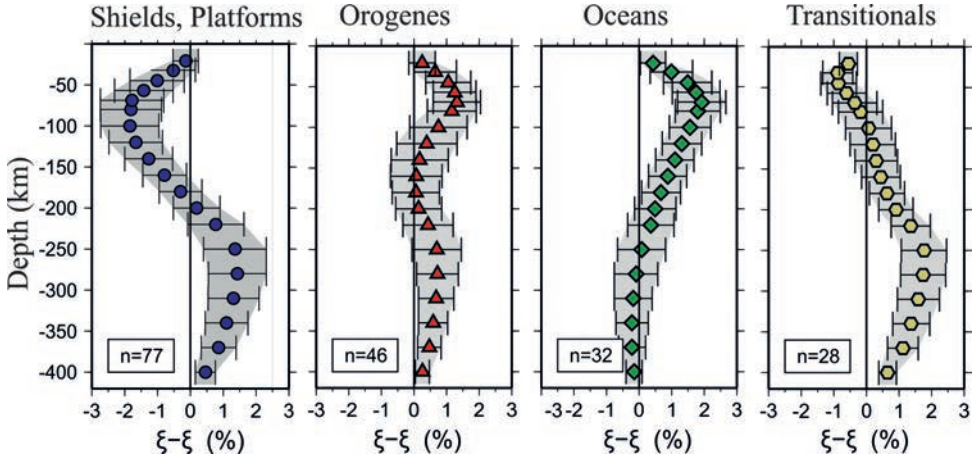

Fig. 6 - Systematic deviations of radial anisotropy found for model of Montagner and Tanimoto (1991) with ~2% radial anisotropy down to 200 km depth (Montagner and Anderson, 1989). The depth-dependent characteristics change according to age of the plates (Babuška *et al*., 1998).

The characteristic depth variations of radial and azimuthal anisotropy can be used for the LAB depth estimates. For example, Burgos *et al*. (2014) and Montagner and Burgos (2019) assign the LAB depth beneath oceans according to three parameters: depth of the maximum in the negative gradient of the shear velocity, depth of the maximum in the positive gradient for

the radial anisotropy, and depth of the correlated layer between the plate motion and azimuthal anisotropy. Beneath the continents, the lithosphere anisotropy is more complex. Therefore, our LAB estimate does not exploit only one of anisotropic parameters of the V_S velocities, but combines both the radial and azimuthal anisotropy. We estimated the global model of LAB (Plomerová *et al*., 2002b), as a depth of a transitional layer between the fossil anisotropy in the lithosphere and anisotropy related to the present-day flow in the sub-lithospheric mantle. Fig. 7 summarises the principles of the LAB depth estimates. We searched for a change in orientation of azimuthal anisotropy or a change in its strength at depths according to characteristic depth-dependences of the radial anisotropy. The LAB depth is associated with the azimuthal-anisotropy change between the minimum and maximum of relative radial anisotropy in regions with the Precambrian characteristic of the mantle lithosphere, between two positive maxima in regions with the Phanerozoic characteristic of the continental mantle lithosphere and around the positive maximum of radial anisotropy beneath the oceans. The proposed global model shows the deepest

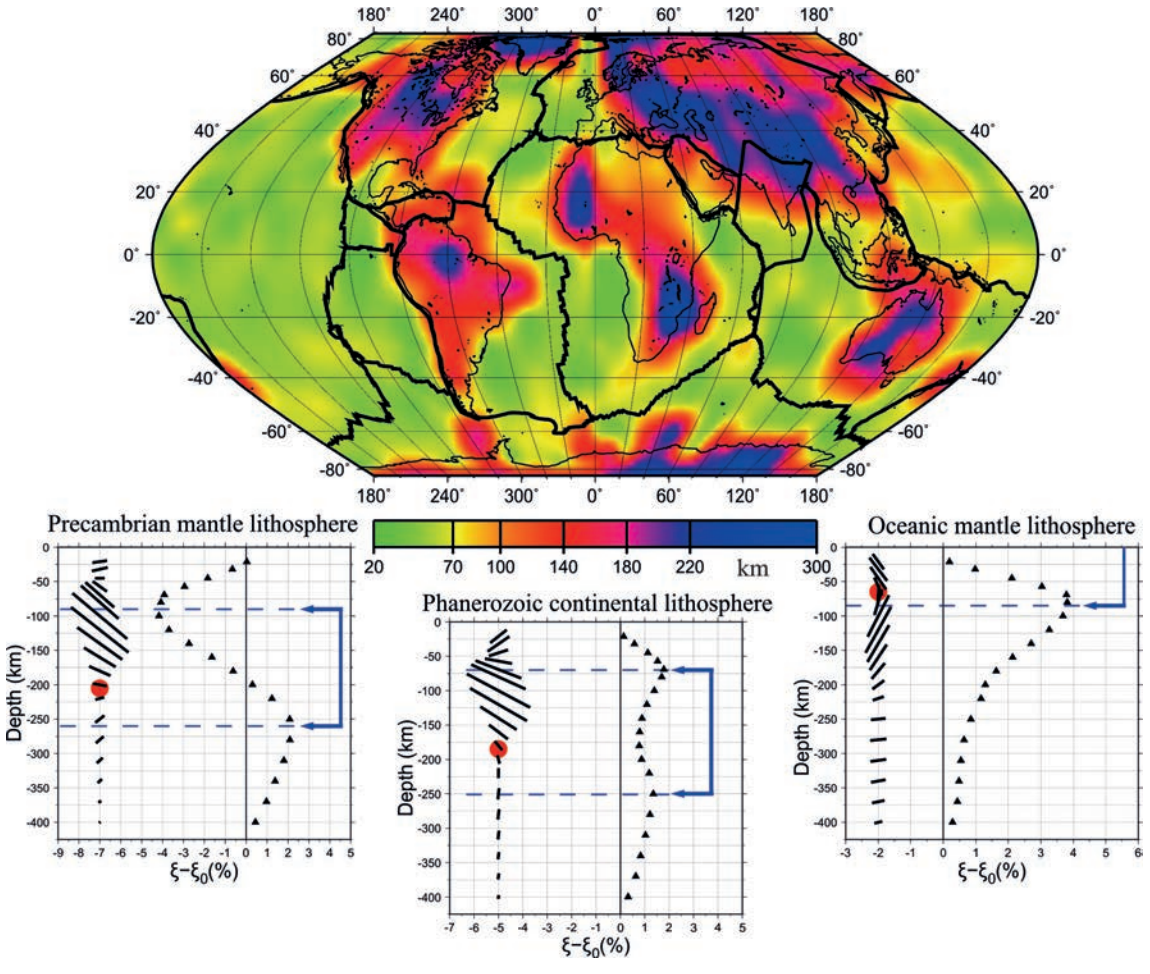

Fig. 7 - Global model of the LAB depth (Plomerová *et al*., 2002b) derived jointly from the azimuthal and radial anisotropy of surface waves and examples of the depth estimates for three tectonically different regions with different characteristics of depth dependence of the radial anisotropy.

LAB at 200-250 km beneath the Precambrian shields and platforms (e.g. Canadian or Baltic shields or, Kaapwal and West African cratons), as well as beneath several collision zones in Asia. The depth of the discontinuity decreases to about 100 km, on average, for the Phanerozoic continental regions, and to 40-70 km beneath oceans.

Questions about the relationship between the lithosphere thickness and its age arise frequently. They concern formation of the lithosphere and reflect how we understand, or we do not, the LAB, regardless of its definitions or visualisations. The oceanic lithosphere originates at ocean ridges and the LAB forms at the bottom of the plates, which thicken away from the ridges. Auer *et al*. (2015) summarised the LAB-depth estimates beneath oceans from different methods against the age of oceanic lithosphere. The zone with a high radial anisotropy, whose upper and lower boundaries coincide with discontinuities imaged by the SS precursors (Schmerr, 2012), appears to be independent of the ages of the Pacific see floor (Fig. 8) (Beghein *et al*., 2014; Burgos *et al*., 2014). However, a change seems to occur around 75 My also in our model, though one has to consider the lower resolution due to the smaller amount of data and possible effects of subduction zones at the ocean margins. Burgos *et al*. (2014) show significant differences of the LAB depth - lithosphere age gradient in dependence on parameter used for the estimate. The authors clearly demonstrate the complexity of the problem even beneath oceans, where the structure of the lithosphere is simpler in comparison with continental plates. Nevertheless, none of the oceanic plates represent a single layer, but their structure shows a stratification between the Moho and LAB (Montagner and Burgos, 2019).

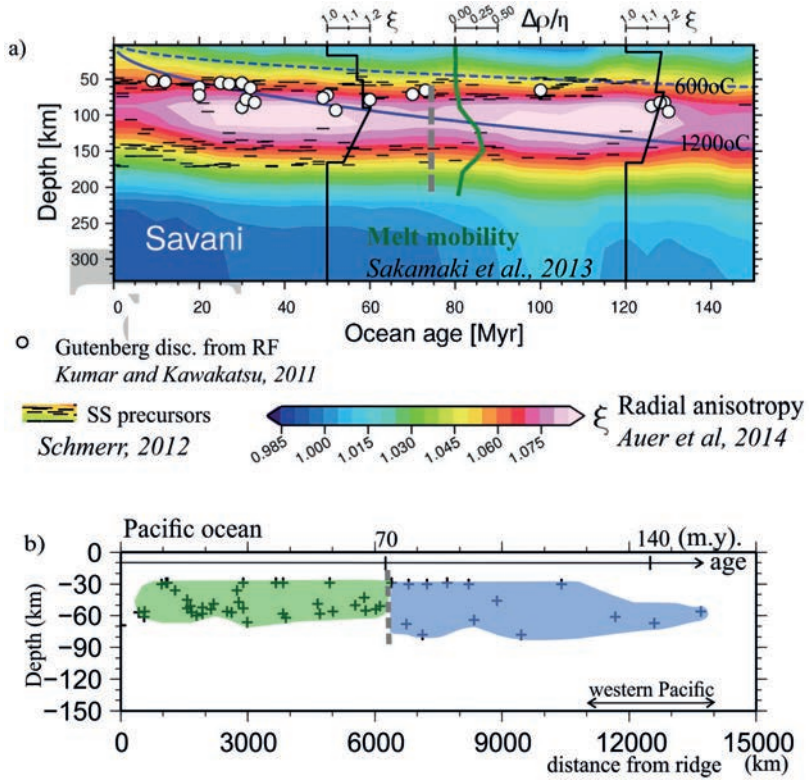

Fig. 8 - a) Summarised observations of the LAB depth beneath oceans (after Auer *et al*., 2015); b) the LAB depth from our model (Fig. 7) as a function of the Pacific seefloor age.

3.2. LAB models from body waves

The advantage of methods using surface wave parameters resides in their vertical resolution, but, on the other hand, they suffer from significant lateral smearing due to the path-integrated effect, which prevents mapping smaller-size structures, particularly in continental regions, with complex tectonics. Teleseismic body waves, propagating steeply upwards through the upper mantle beneath target regions, allow us to search for lateral variation of LAB relief and other discontinuities in general at shorter scales. They carry information which can be exploited for mapping the Earth discontinuities with larger lateral resolution in comparison with surface waves, though with limited vertical resolution.

3.2.1. Discontinuity imaging by converted phases

Recently, body-wave phases converted at the Earth discontinuities, particularly the shear-to-longitudinal phases in case of the LAB and MLD (e.g. Rychert and Shearer, 2009; Abt *et al*., 2010; Kind and Yuan, 2019; Rychert *et al*., 2019), have become one of the most frequently used methods to image the upper mantle discontinuities. Because the amplitudes of the converted phases are one order lower than the amplitude of the incoming wave, isolating the converted phases requires processing of a large amount of waveforms. Moreover, the results are usually presented in bands of several hundred kilometre broad, which also limits the lateral resolution of these methods, regardless of the polluting effects of individual approaches (side-lobs). Methods utilising the converted phases image flat or moderately dipping discontinuities/narrow transitions, across which velocities significantly change. From the dependence on these criteria one can judge sharpness of the discontinuities, in a sense of width of the transition and size of the velocity "step". The converted-wave methods highlight the Earth discontinuities and reveal several new regional interfaces within the upper mantle (e.g. Kind *et al*., 2017). The new discontinuities add new constraints to a more detailed understanding of plate collisions. Thus, for example, suggested penetration of the cratonic mantle lithosphere into the Phanerozoic asthenosphere, during the continental collision at the south-western edge of the East European Craton (EEC) in central part of the Trans-European Suture Zone, agrees well with inferences from body-wave anisotropy (Vecsey *et al*., 2014; see also Section 3.2.3 here).

S-to-P converted phases are very efficient in imaging the MLD, one of the most significant interfaces for understanding the structure of the Precambrian lithosphere. The MLD occurs beneath the Precambrian units at about ~90 km depth, which is similar to the LAB depth beneath the Phanerozoic regions, while the cratonic LAB is significantly weaker and deeper (Kind and Yuan, 2019). Similarly to PS phases, the strongest SP phases are generated at the Moho, the discontinuity between the crust and mantle, and then at the 410 and 660 km discontinuities marking the upper/lower mantle transition zone.

3.2.2. Body-wave anisotropy approach to image LAB

Various techniques of body-wave receiver functions emphasise the velocity contrasts at certain depths. But the teleseismic body waves propagate through the upper mantle and sample the velocity structure in the entire volume along their paths. By analysing the relative travel times, a volume with higher velocities can be identified in the sub-lithospheric mantle (asthenosphere). Based on variations of directional terms of relative P-wave residuals presented in P spheres and SKS-wave

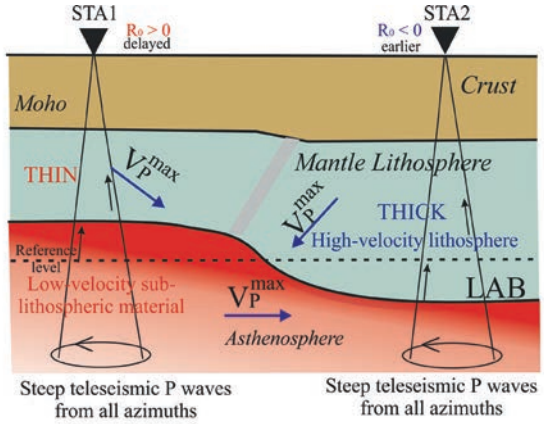

Fig. 9 - Cartoon of the LAB depth estimate from static terms of relative P-wave residuals R_0, corrected for crust structure, deep mantle path, and source side effects. Inclined fabrics of the mantle lithosphere increase velocity contrast across the LAB discontinuity.

splitting, we have been studying structure of the continental lithosphere, mostly of the European plate, since early 1980s. Our results document that the lithosphere is a mosaic of amalgamated plate fragments with their own fossil fabrics (e.g. Babuška *et al*., 2002; Plomerová and Babuška, 2010). Fabrics of the individual mantle-lithosphere domains modelled in 3D are inclined and can be approximated by anisotropic aggregates with plunging symmetry axis - high velocity lineation or dipping foliations. Then, steep teleseismic P waves propagate in directions close to lower velocities beneath the lithosphere and along the higher velocities with the lithosphere (Fig. 9). Different orientations of anisotropy in the lithosphere (inclined high velocities) and the asthenosphere (high velocities mostly sub-horizontal) increase the velocity contrast across the LAB.

Adopting the lithosphere as a high-velocity portion of the outer shell of the Earth, regions with a thick lithosphere exhibit relatively early P-wave arrivals on average (Fig. 9), because of an abundance of the high-velocity material in comparison with the radial Earth velocity models. The P-wave arrivals in regions with a thin lithosphere are delayed due to the lack of the high-velocity material in the lithosphere. To model lateral variations of the depth of the lithosphere-asthenosphere transition, we isolated at each station static terms of relative residuals (calculated from steep rays arriving from all azimuths), which have been corrected for effects from the crust and source-sides (including locations), as well as from heterogeneities along the deep mantle paths. To relate the travel-time differences with lateral variations of the lithosphere thickness, we derived an empirical gradient dH/dR_0 = 9.4 km/0.1 s (Babuška *et al*., 1984) by associating the thickest lithosphere in the central part of the western Alps (~220 km) and the shallowest LAB in the Belgo-Dutch platform (~50 km) (Baer, 1980; Mueller, 1982) with the most negative (-1.0 s) and positive static terms (+0.8 s) of relative P-wave residuals, carefully calculated for European stations. No other assumptions were made.

Is it possible to explain the empirically set gradient, which requires a velocity contrast of ~0.6 km/s? Babuška and Cara (1991) compared variations of mean P-wave velocities of the upper-mantle rocks due to changes in composition and anisotropy. The comparison clearly documents that anisotropy has a similar, or even larger, impact on velocity variations than the

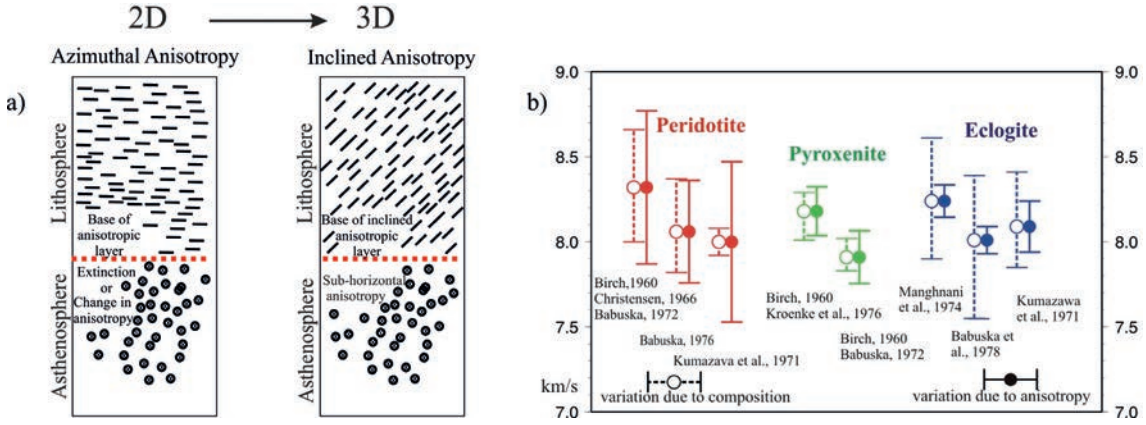

Fig. 10 - a) Schematic representation of 2D and 3D view of lithosphere and asthenosphere fabrics; b) variations of the mean P velocities due to composition and anisotropy of the upper mantle rocks, measured under 0.5-1.0 GPa (Babuška and Cara, 1991). Average composition of the upper mantle is about 60% of peridotite, 30% of pyroxenite and 3% eclogite.

mineral composition (Fig. 10b). Assuming mantle composition and the P anisotropy of peridotite xenoliths at 9-10% and S anisotropy at 6-7% (Ben-Ismail and Mainprice, 1998), then velocities for sub-vertical propagations within the mantle lithosphere with ~45° dipping foliation are ~8.25 km/s and 7.70 km/s in the sub-lithospheric mantle, characterised mostly by sub-horizontal high velocities (Fig. 10a). Even if we consider an additional 0.1 km/s reduction due to a possible partial melting at the bottom of the lithosphere, we end up with a velocity contrast of ~0.65 km/s across the LAB. Such a velocity drop of ~8% results in dH/dR_0 = 9.6 km/0.1 s, which is even larger than the empirically derived gradient of the time residual - LAB depth relation. However, the anisotropy measured on xenoliths reflects the structure of laboratory samples. The large-scale anisotropy reflects the amount of alignment of olivine crystals (LPO) in a large volume and represents the dominant source of velocity anisotropy in the mantle. Anisotropy strength in the upper mantle scanned with seismic waves could be about 2/3 lower than the anisotropy of peridotite measured on mantle xenoliths, but still remaining strong enough to compete with velocity variations caused by mineralogical and/or temperature heterogeneities. Nevertheless, the ~8% velocity drop is fully compatible with inferences published in a review by Fischer *et al*. (2010) based on estimates of relations of SP amplitudes, velocity drops, the discontinuity "widths" and wavelengths.

3.2.3. European LAB

Even first application of the empirical gradient mapped effectively the relief of European LAB (Babuška *et al*., 1984, 1987) and indicated a separation of the lithosphere roots of the western and eastern Alps. At that time, the deep lithosphere root, resulting from the Eurasian - African plate convergence, was considered as a single bent root that mimics the surface shape of the mountain crest. By complementing parametric ISC data (ISC bulletins) with P arrival times from several regional networks [e.g. Swiss Seismological Service (Baer, 1980), Eastern Alpine Network (Aric *et al*., 1989)] we were able to model the LAB and calculate tomography images of the upper mantle in greater detail (Babuška *et al*., 1990). Both the map view of the LAB relief (Fig. 11a) and the velocity perturbations in a 85 km thick layer below the Moho, clearly show separation of the two

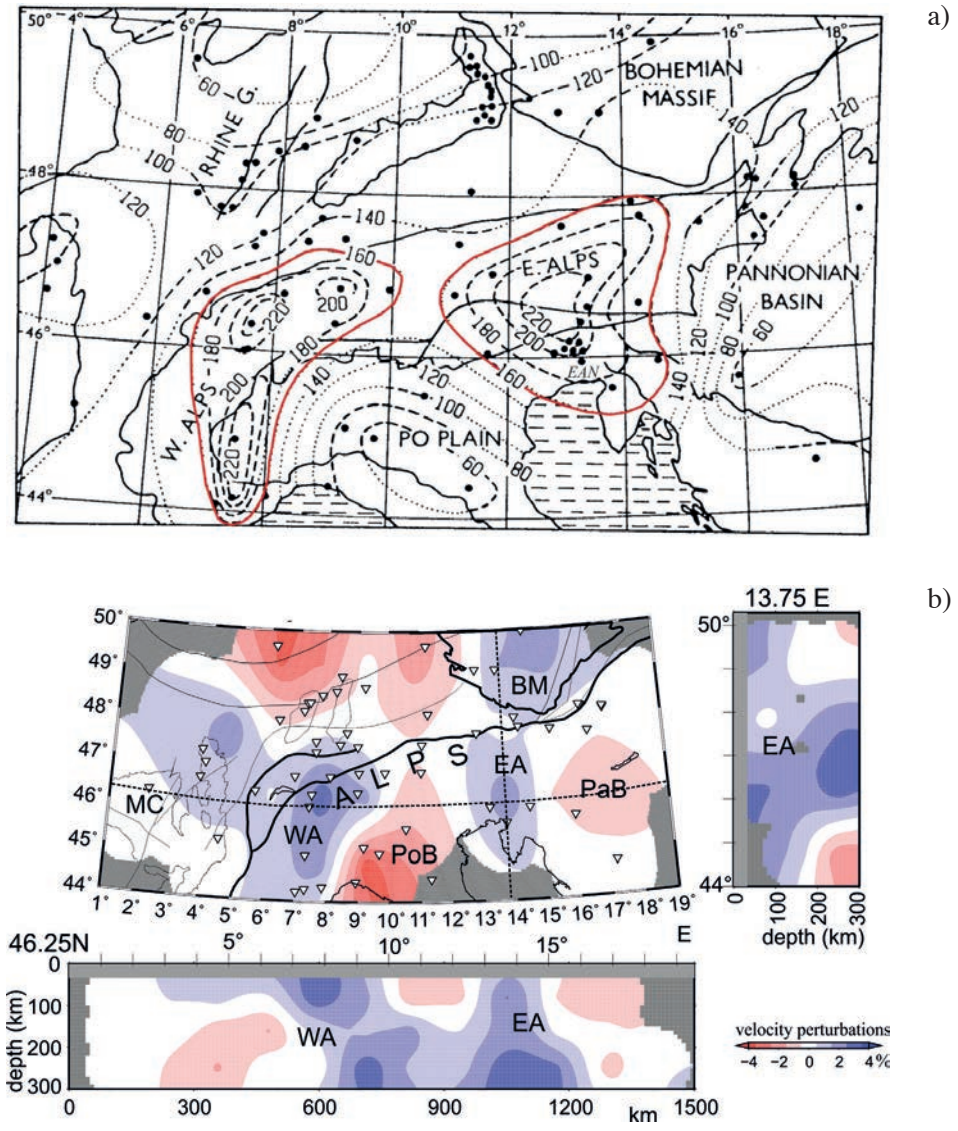

Fig. 11 - a) LAB model around the Alps showing two separate roots of different geometry (Babuška *et al*., 1990); b) velocity perturbations of standard isotropic tomography at 85 km thick layer below Moho showing separation of lower lithosphere roots in the western (WA) and eastern (EA) Alps, their different shapes and switched polarity of the subductions (redrawn according to Babuška *et al*., 1990). MC-French Massif Central, BM - Bohemian Massif, PoB - Po Basin, PaB - Pannonian Basin.

lower lithospheric roots, their different shape and the switched polarity of the subductions (Fig. 11b). While the bent rim of the European plate in the western Alps subducts regularly to the east, the European - Adriatic plate convergence in the eastern Alps is much steeper northwards and more complex. Tomography studies based on data from regional passive seismic experiment organised later in the Alps (TRANSALP: Transalp Working Group, 2001) imaged similarly two separated mantle roots beneath the western and eastern Alps (Lippitsch *et al*., 2003) with switched polarities.

Station distribution in most of Europe is sufficiently dense to map undulated relief of the LAB, especially thanks to passive seismic experiments in northern Europe, namely TOR [1996-

1997: e.g. Gregeresen *et al*. (2002)], SVEKALAPKO [1998-1999, e.g. Sandoval *et al*. (2004); Hjelt *et al*. (2006)], LAPNET [2007-2009: e.g. Silvennoinen *et al*. (2014)]. Some complementary information on the LAB relief in central Europe was obtained from temporary arrays BOHEMA I-IV [2001-2006, 2014-2015: e.g. Plomerová *et al*. (2007)], RETREAT [2003-2006: Plomerová *et al*. (2006)], ALPASS [2005-2006: Mitterbauer *et al*. (2011)], PASSEQ [2006-2008: Wilde-Piorko *et al*. (2008)] or CBP [2005-2008: e.g. Dando *et al*. (2011)]. Fig. 12a shows current status of our model of the LAB based on data from permanent observatories and previous passive seismic

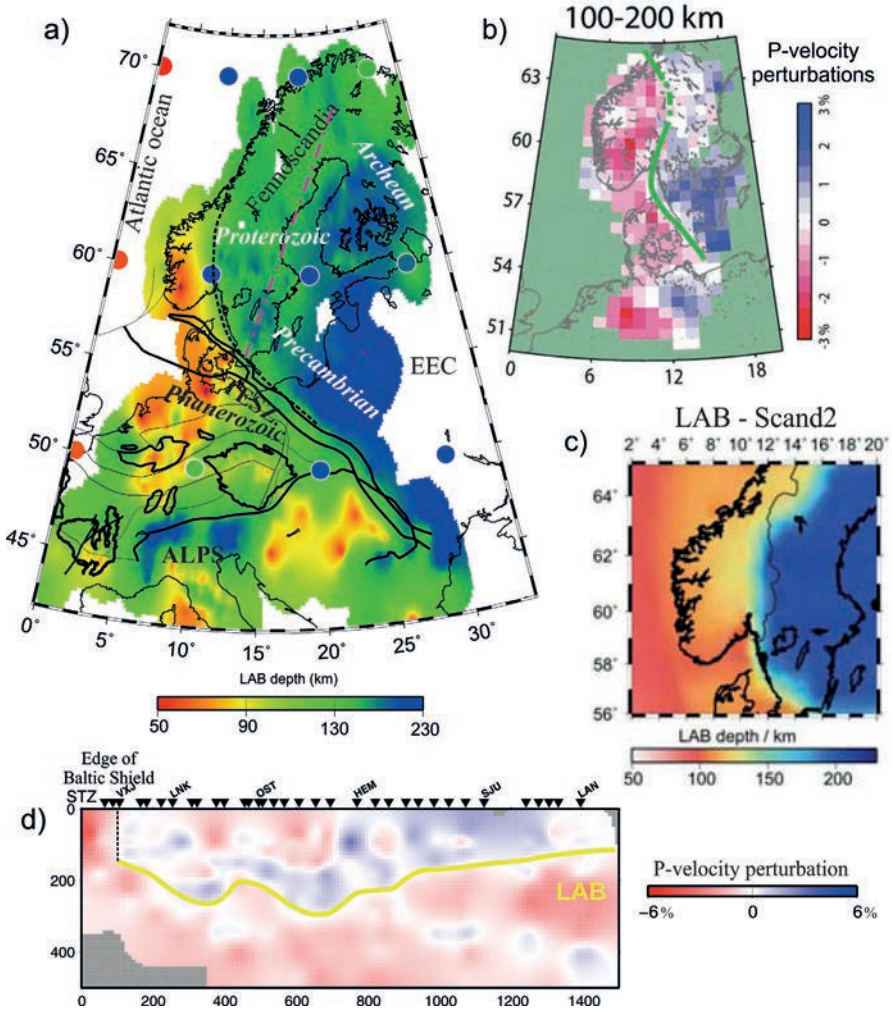

Fig. 12 - a) European LAB depth derived from static terms of relative P-wave travel time deviations (see Fig. 9), along with values from the global model of LAB from radial and azimuthal anisotropy of surface waves (circles, see also Fig. 7). The dashed line contours the thick Baltic shield lithosphere; b) the south-western edge of the thick shield lithosphere (green line) in the P-wave travel time tomography (Medhus *et al*., 2012) based on data integrated from the CALAS, MAGNUS, SCANLIPS, GENMOVE, and TOR passive seismic experiments; c) the shield edge as in integrated geophysical Scand2 model (Gradmann *et al*., 2013) with the use of LitMod3D code (Afonso *et al*., 2008; Fullea *et al*., 2009), showing an abrupt change in the lithosphere thickness between southern Norway and southern Sweden; d) SW-NE cross-section (the profile marked in panel a) showing the edge of the shield and the lithosphere thickening towards its central part, followed by a thinning further to the north, in teleseismic P-wave tomography from data of the Swedish National Seismic Network (SNSN) (after Eken *et al*., 2012).

experiments. The thin lithosphere ~60 km is modelled beneath the Pannonian Basin, Po Plain, the southern part of the French Massif Central, Rhenish Massif, Denmark and the south-western rim of Fennoscandia. In addition to the Alpine roots, the lithosphere thickens up to 220 km beneath large parts of the Fennoscandia and western EEC. The LAB beneath the Phanerozoic part of Europe is, in general, shallower and relief is greater than that beneath its Precambrian part.

Several studies have tried to identify the south-western edge of the Baltic Shield with the use of different methods and data (Fig. 12b). The deep and narrow boundary between areas of contrasting upper-mantle P-wave velocity structure has been detected in different teleseismic P-wave tomography (e.g. Medhus *et al*., 2012; Eken *et al*., 2012) and was related to the south-western edge of the thick shield lithosphere. Integrated geophysical modelling [LitMod3D: Afonso *et al*. (2008); Fullea *et al*. (2009); Gradmann *et al*. (2013)] favour a model with the abrupt change in the lithosphere thickness between southern Norway and southern Sweden as well. The distinct change of the LAB is recorded also in our global model from surface wave anisotropy [Plomerová *et al*. (2002b), see also Fig. 7].

Distinct LAB-depth variations over short lateral distances were detected in several other European regions by utilising data recorded at dense arrays. For example, the closely spaced stations in the TOR experiment provided recordings, on the basis of which we modelled the LAB depth variations from the North German Basin with thin lithosphere, across Denmark towards southern Sweden with ~200 km thick lithosphere. The LAB depth changes are not smooth, but step-like and they relate to significant sutures: the Thor Suture (TS) and Sorgenfrei-Tornquist Zone (STZ) (Fig.13). The LAB relief, modelled as a transition between the fossil anisotropy in the mantle lithosphere and anisotropy related to present-day flow in the sub-lithospheric upper mantle is compatible with results from surface waves or body-wave isotropic velocity tomography, though the latter have a lower lateral resolution. Our model of the continental mantle lithosphere consists of anisotropic domains with different fabrics and thicknesses. The depth of the lower boundary of the domains, the LAB, the world-wide discontinuity, does not change smoothly.

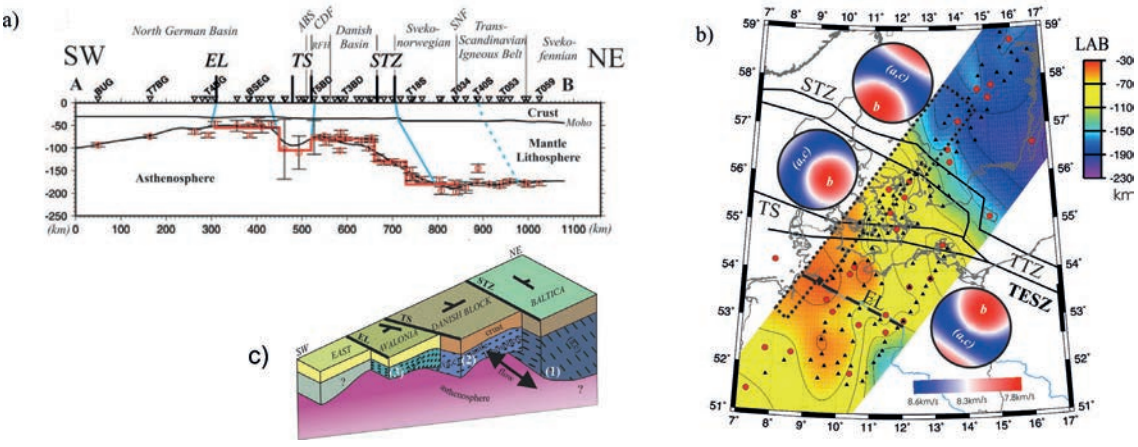

Fig. 13 - a) Cross-section showing the step-like thinning of the lithosphere across the Sorgenfrei Tornquist Zone (STZ) and the Thor Suture (TS), delimiting the mantle-lithosphere domains with their own fabrics (see the region framed by dotted lines in panel b for location); b) map view (after Plomerová *et al*., 2002a); and c) cartoon illustrating individual blocks of the lithosphere (after Babuška and Plomerová, 2004).

There are vertical "discontinuities" (steps) of this transition due to the thickness variability of sharply bounded domains of mantle lithosphere.

The Trans-European Suture Zone (TESZ) is the most dominant suture zone separating the Phanerozoic and Precambrian parts of Europe, in which the LAB exhibits different characteristics. While the LAB changes in a step-like manner across the north-western part of the zone (see Fig. 13), in the central part of TESZ (Poland) the LAB depth increases smoothly across the Teisseyre-Tornquist Fault Zone (TTZ), marking the surface trace of the north-western extent of the EEC. Anisotropy studies of the upper mantle around the TESZ showed that neither the fabrics derived from SKS splitting (Vecsey *et al*., 2014) nor those from P waves change suddenly (Fig. 14), as it happens around the north-western part of the TESZ (Plomerová *et al*., 2002a). We interpret the continuation of the Precambrian anisotropic characteristics across the TESZ further to the SW as an over-thrusting of the Phanerozoic units above the Precambrian mantle lithosphere of the ECC, which is in agreement with tomography images of the upper mantle velocities (Chyba *et al*., 2017) (Fig. 14). SP conversions (Kind, 2017) detected an interface steeply dipping beneath the Bohemian Massif at depth below 200 km. The author related the interface to a continuation of the

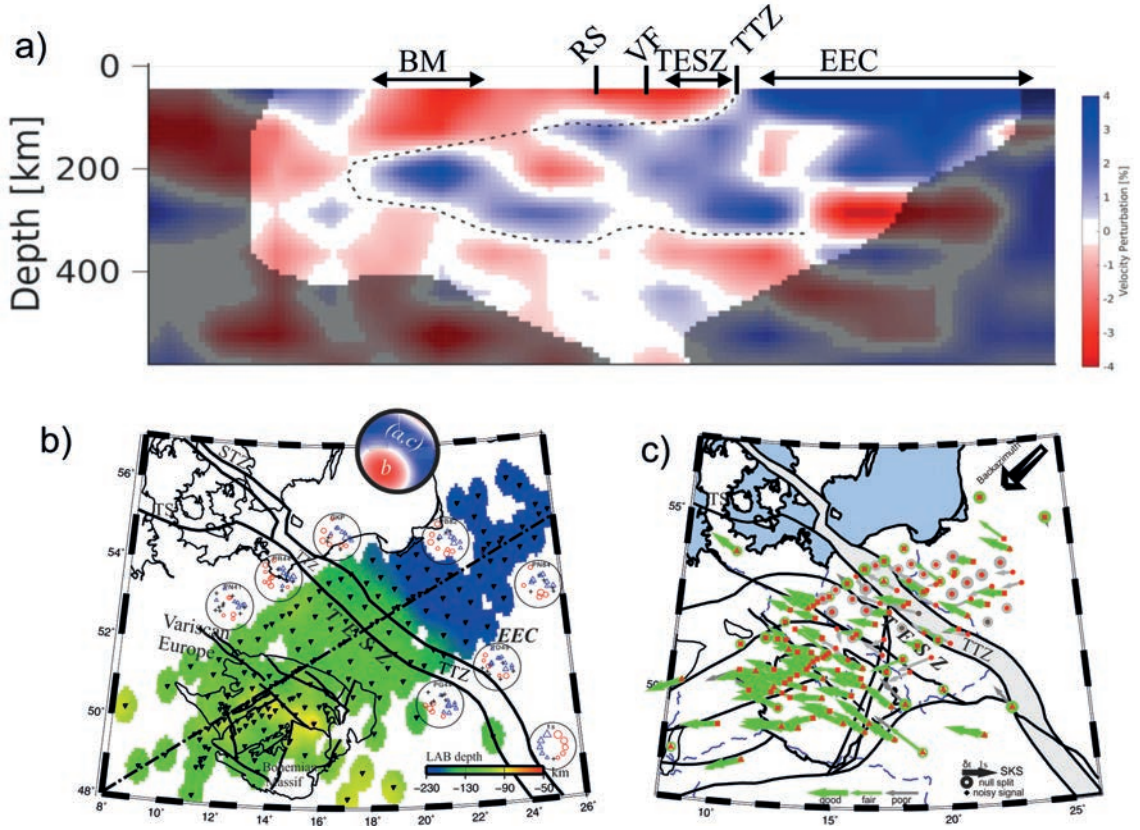

Fig. 14 - a) Cross-section through teleseismic P-wave tomography (Chyba *et al*., 2017) along the SW-NE profile across the TESZ, calculated from data of the PASSEQ seismic experiment [stations plotted in part (panel b) with a model of LAB depth]. No significant change in anisotropic signals related to the TTZ in the P waves (panel b) neither in the shear-wave splitting (panel c) supports a penetration of the EEC further to the SW (the contoured high velocity perturbations in panel a).

cratonic LAB of the EEC. Thus, inferences from body waves support those from our anisotropy studies from surface waves, which indicate the larger extent of the Precambrian mantle lithosphere in comparison with the extent of the Precambrian crust (Babuška *et al*., 1998; Plomerová *et al*., 2002b).

Similar unit contacts were modelled in northern Fennoscandia where the Archean domains penetrate into the Proterozoic units towards the west both from data of the LAPNET (northern Finland) and SVEKALAPKO (south-central Finland) experiments (Fig.15). The wedge-like structure of the mantle lithosphere around the Archean/Proterozoic contact in the south-central Finland (SVEKALAPKO experiment) is supported by the alternating Proterozoic - Archean - Proterozoic ages of kimberlites (Peltonen and Brügmann, 2006) as well as by shear-wave velocities in surface wave tomography (Funke *et al*., 2003; Hjelt *et al*., 2006). The LAB shallows northwards in our model of the Baltic shield (Plomerová *et al*., 2008) in agreement with the results of velocity models derived from surface waves (Pedersen *et al*., 2013) or teleseismic P-wave tomography (Silvennoinen *et al*., 2016). Also, novel anisotropic tomography code (Munzarová *et al*., 2018a) applied on the LAPNET data revealed domains in the mantle lithosphere with different fabrics (Munzarová *et al*., 2018b).

Phanerozoic Europe contains several Variscan massifs (Fig. 16), whose structure and depth extent have been the subjects of several studies in the past (e.g. Barruol and Granet, 2002; Judenherc *et al*., 2002; Walker *et al*., 2004; Schulmann, 2009). Granet *et al*. (1995) postulated a theory that the LAB and the massifs are disrupted by baby plumes, which have a common origin at greater depth (Fig. 16). Such a baby plume affects the southern block of the eastern part of the French Massif Central (MC) (Fig. 17), where the LAB shallows at least up to ~60 km, while the LAB of the western domain (Limousin) and the northern block of the eastern part of the MC reside at 120-140 km depth (Babuška *et al*., 2002), typical for the massifs (see Fig. 12a). Similar LAB disruption and lithosphere thinning were modelled beneath the Rhenish Massif (Ritter *et al*., 2001; Walker *et al*., 2004). On the other hand, the Armorican Massif in western Europe did not suffer from any significant thermal event at all. The complex structure of the massif, formed by a collage of several accreted continental and oceanic pieces, is cut by two prominent sutures - South and North Armorican Shear Zones - along which the hot asthenospheric material could be transported to the surface. The LAB depth is estimated at ~140-150 km (Judenherc *et al*., 2002; Artemieva, 2018).

The Bohemian Massif (BM) in central Europe is the largest of the Variscan massifs (see Fig. 16) and thanks to several passive seismic experiments that covered the region since early 90th, the lithosphere discontinuities and its structure could be studied in detail. The LAB maintains ~120 km depth on average; it thickens beneath the Moldanubian unit (MD), reflecting the Brunovistulian (BV) domain underthrusted from the east and shallows locally along boundaries of the mantle-lithosphere domains. The lithosphere thins along the Saxothuringian (ST)/Teplá Barrandian (TB) contact, the Eger Rift (ER), the contact of Sudetes (SU) with the Silesian (SI) and Brunovistulian units, or, beneath the Kozákov Tertiary volcano (Fig. 18). The sutures beneath the mantle-lithosphere domains and faults served as paths for transport of the mantle material to the surface (Babuška and Plomerová, 2013). Volumes of the mantle domains, each of them with its own consistent dipping fabric (Fig. 18c), were revealed from body-wave seismic anisotropy and the domain boundaries set according to changes of their fabrics. The shallowest LAB was found along the Eger Rift in the western part of the massif, where also a baby plume was formerly

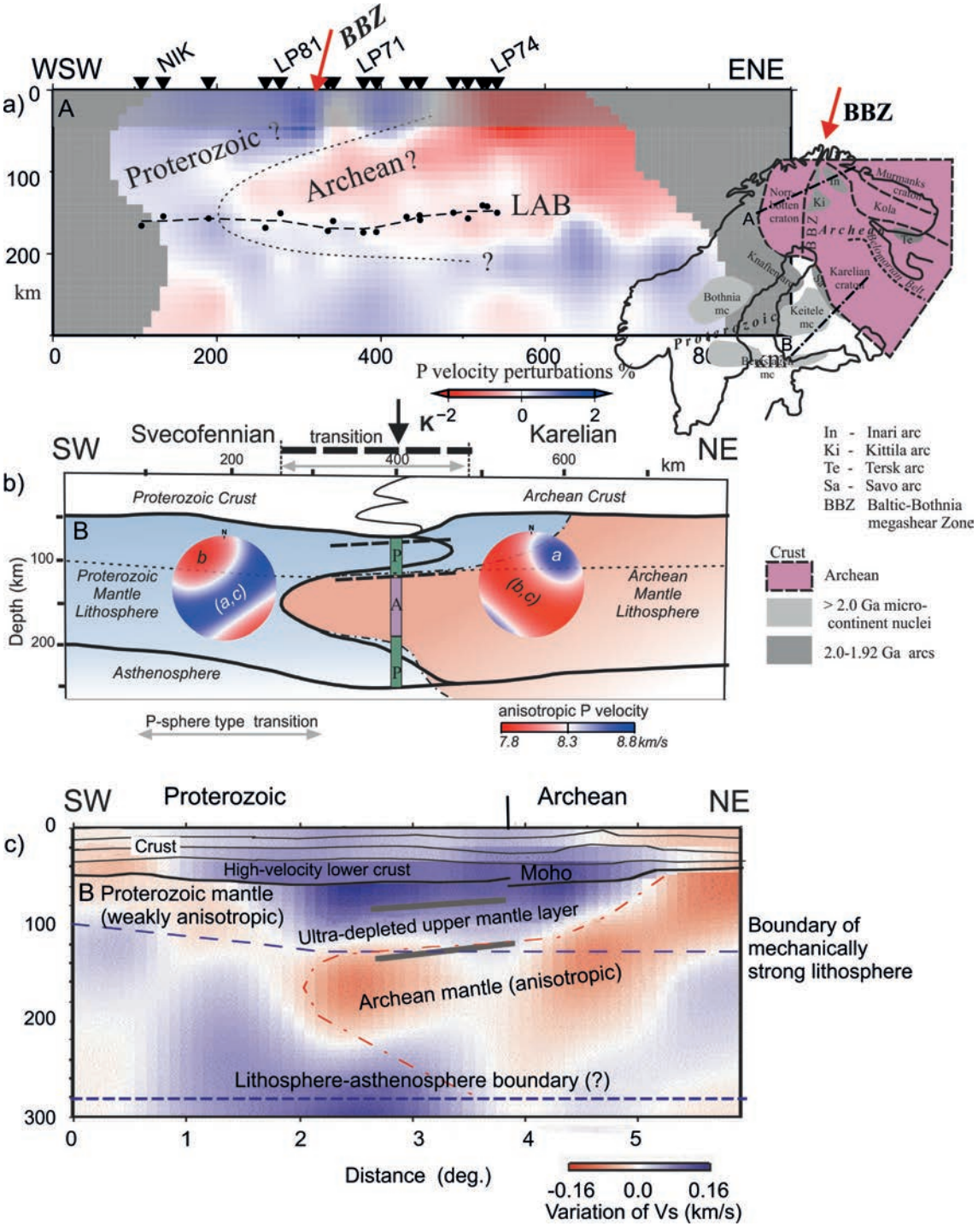

Fig. 15 - Wedge-like contact of the Archean and Proterozoic domains: a) the north-eastern Fennoscandia in teleseismic P-wave tomography; b) south-central Finland from anisotropy studies (Plomerová *et al*., 2006; Vecsey *et al*., 2007); c) from surface wave tomography by Funke *et al*. (2003) (redrawn form Hjelt *et al*., 2006). K- the Kaavi-Kuopio Kimberlite Province, mantle xenoliths of the Proterozoic (green) and Archean (violet) ages according to Peltonen and Bruegmann (2006).

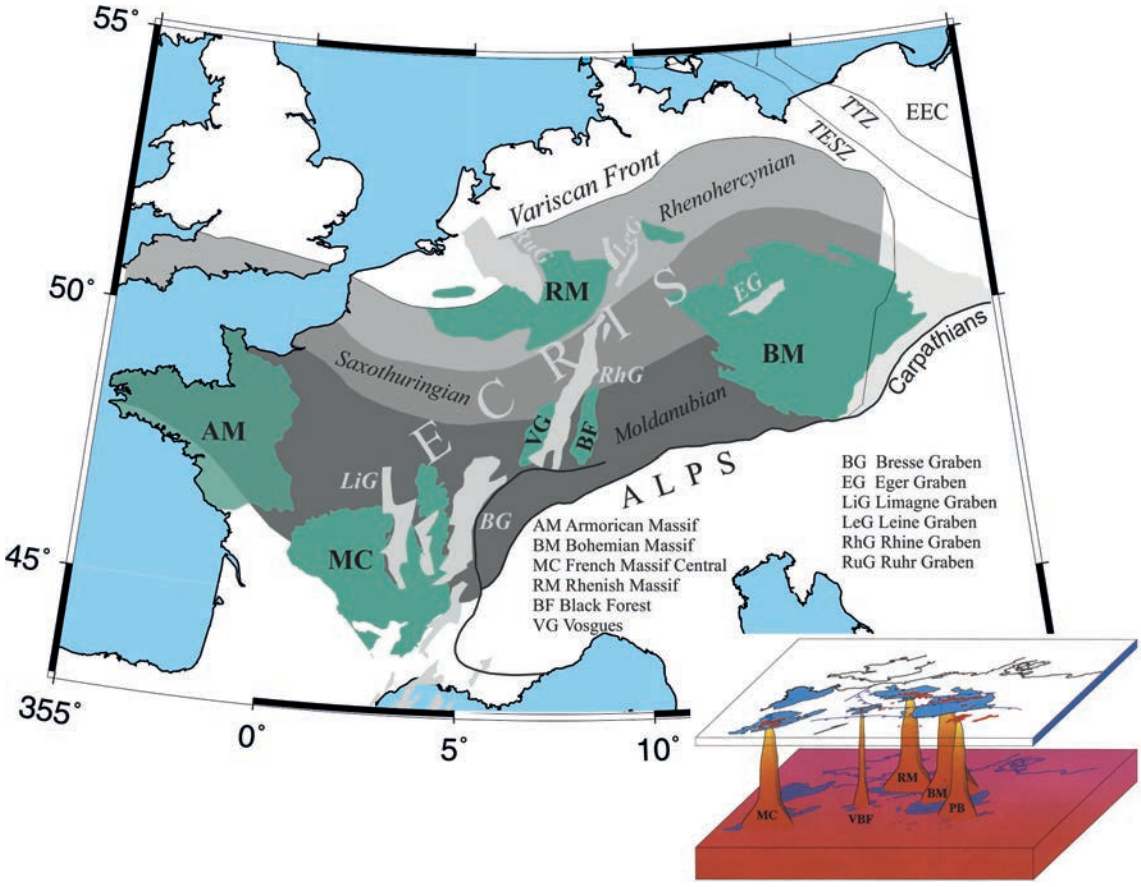

Fig. 16 - Variscan orogenic belt, massifs and European Cenozoic Rift System (ECRIS). The baby plume concept after Granet *et al*. (1995).

advocated beneath the south-western end of the Eger Rift (see Fig. 16). The BOHEMA experiment, targeted at confirming the existence of the narrow baby plume beneath the western BM, did not evidence the presence of such plume, analogous to those beneath the MC or RM (Granet *et al*., 1995; Ritter *et al*., 2001). Instead, we inferred there a broad LAB upwelling, due to an erosion of the steep ST and TB domain boundaries at depth (Plomerová *et al*., 1998, 2007, 2016; Babuška and Plomerová, 2017).

Modelling the LAB discontinuity beneath younger orogenic regions is more difficult, but still provides realistic images, if proper crustal corrections are applied. A passive seismic experiment AlpArray (Hetényi *et al*., 2018a) and its complementary component AlpArray-EASI provided data for a detailed study of the crust (Hetényi *et al*., 2018b) and the upper mantle beneath the central Europe, particularly in a band across the western BM and the eastern Alps. The European plate thickens from ~80 km beneath the ER southwards to ~160 km (Fig. 19) in the contact zone with the steeply northward dipping Adriatic plate, which has been imaged also in different velocity tomography models of the upper mantle (Babuška *et al*., 1990; Karousová *et al*., 2013). Reversed patterns of the European- and Adriatic-plate fabrics affect modelling the LAB in the vicinity of the contact zone, around 47.3 N. Because the majority of rays propagate along the

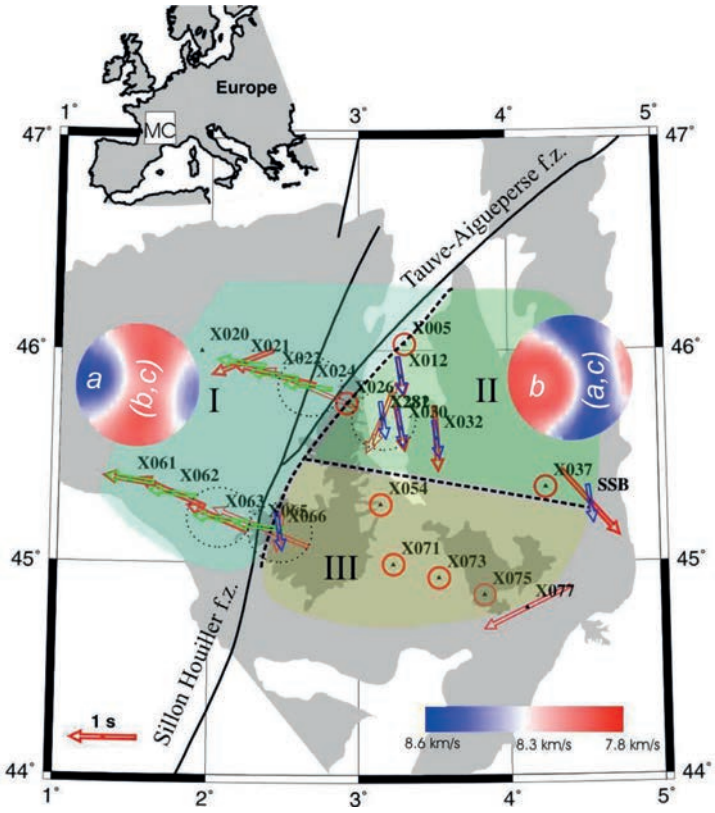

Fig. 17 - The lithosphere model of the French Massif Central. The three domains differ in the LAB depth and exhibit their own fabrics. The LAB depth lies at 120~140 km beneath the western and north-eastern domains (domains I and II), and at about 80 km or even less (Sobolev *et al*., 1997) beneath Domain III in the south. Fabric of the mantle lithosphere is modelled by westward dipping lineation in the west from the Tauve-Aiguperse Fault Zone and eastward dipping foliation east of the fault zone. The models are compatible with anisotropic signals from the P-wave travel time deviations and shear-wave splitting (Babuška *et al*., 2002). Green and blue arrows marks down dipping fast S polarisation directions calculated for the models, the red arrows were retrieved from the data.

low-velocity directions, the estimate of the LAB depth is too shallow. On the other hand, the LAB depths beneath the northernmost part of the Adriatic plate might be exaggerated due to the long wave paths along the high velocities within the dipping slab.

The northern Apennines is another orogenic region where we studied the mantle-lithosphere structure and modelled the LAB (Plomerová *et al*., 2006). We revealed a ~50 km shallow oceanic LAB beneath the Tyrrhenian Sea and ~200 km deep Apennines root of the ~80 km thick subducted Adriatic plate (Fig. 20) (Munzarová *et al*., 2013) with the use of the RETREAT experiment data (Margheriti *et al*., 2006). The relief of the LAB discontinuity changes dramatically across the northern Apennines over lateral distance of ~100 km. In the LAB modelling, we have slightly modified the Moho step at the contact of the Tyrrhenian and Adriatic crusts (Di Stefano *et al*., 2011) into an over-/under-thrust shape, which is more likely in such contact zones (Hetényi *et al*., 2018b).

Jones *et al*. (2010) compared statistically LAB depths modelled by different methods, which differ in their accuracy and survey different physical parameters. The comparison showed that in central Europe the seismic $sLAB_{RF}$ from receiver functions (Geissler *et al*., 2010) is 33±18 km shallower, on average, than our seismic sLABa considering anisotropy (Plomerová and

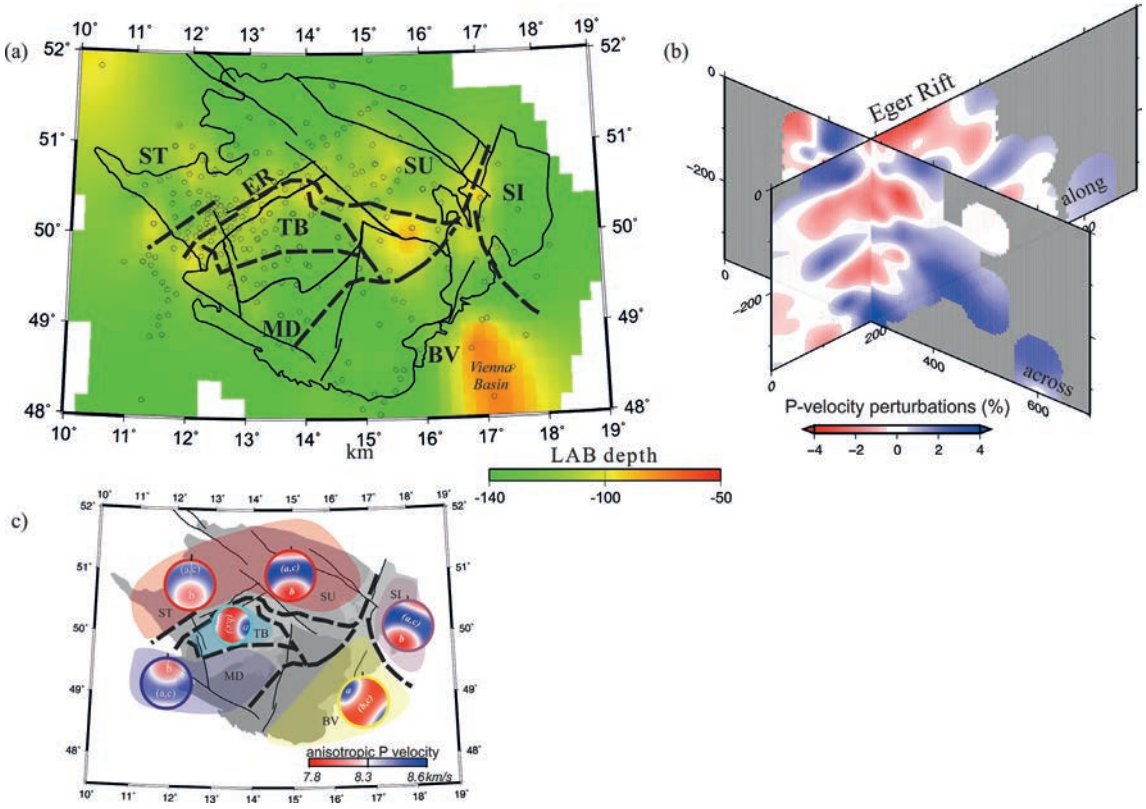

Fig. 18 - Locally thinned lithosphere beneath the Bohemian Massif: a) the LAB relief derived from data of several passive seismic experiments [BOHEMA I-III, ALPASS (northern part), PASSEQ, EgerRift] in the region; b) cross-sections along and across the Eger Rift through the teleseismic P-wave tomography showing the elongated upwelling of the lithosphere instead of a hypothetical (Granet *et al*., 1995) thin tube-like low-velocity associated with the assume baby plume (Plomerová *et al*., 2016); c) fabrics of individual domains of mantle lithosphere and the domain boundaries in depth (dashed curves) (Babuška and Plomerová, 2013). Note the shift between the boundaries in the mantle and surface traces of the crustal units.

Babuška, 2010), except for sites with a thick sedimentary cover. Comparison of electrical (eLAB) and seismic sLABa revealed significant differences between these two estimates in the Phanerozoic and Precambrian parts of Europe. While in the Precambrian Europe the eLAB - sLABa distribution exhibits a single peak at +40 km with a long tail towards the positive values, in the Phanerozoic Europe the distribution is of bi-modal character with peaks at -40 km and +20 km, rapidly decreasing on both sides. Even if we take into consideration differences of the physical parameters of the methods and in their resolution, it is evident that the eLAB and sLABa or $sLAB_{RF}$ do not detect the same interface.

In the estimate of the lithosphere thickness in Europe by Artemieva (2018), the LAB_{topo} is based on analysis of topography deviations from the expected correlation between the Moho depth and topography. Anomalous topography is explained by thermal anomalies in the lithosphere and by variations in the lithosphere thermal thickness. In Precambrian Europe the LAB_{topo} deepens to ~300 km in this model and thus exceeds depth of sLAB, but it lies shallower that in models of the thermal lithosphere thickness, where LAB_T is suggested at depth >300 km for northern Europe (Artemieva and Mooney, 2001).

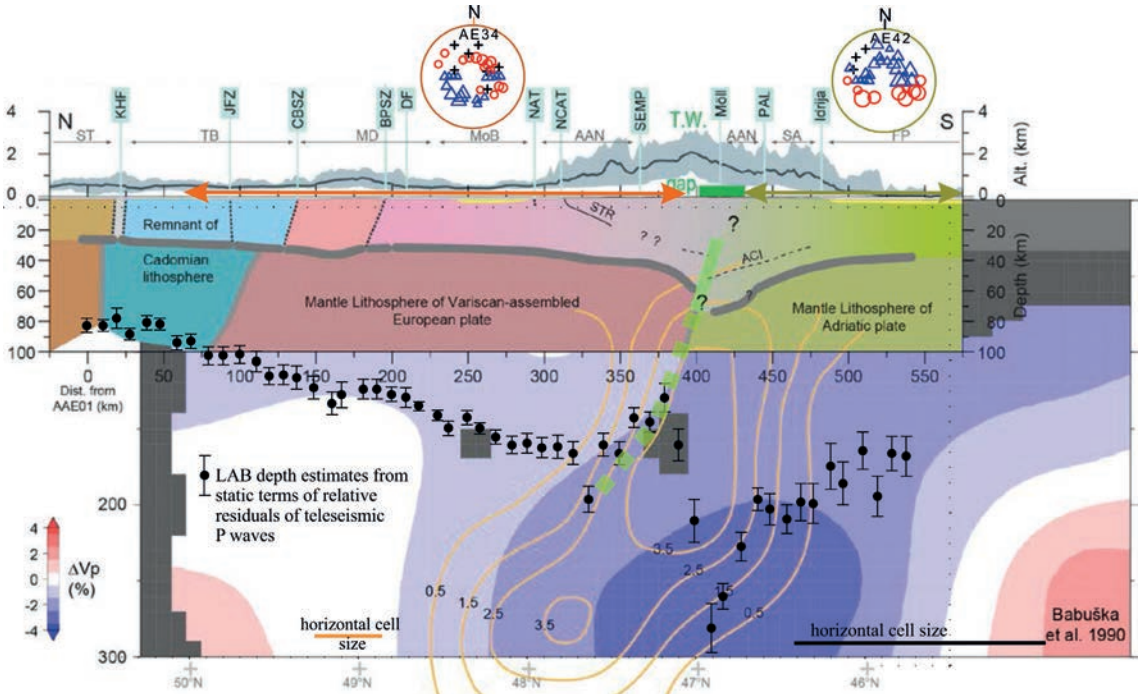

Fig. 19 - The lithosphere structure across the eastern Alps showing the Moho discontinuity from P receiver functions (after Hetenyi *et al*., 2018b) and the LAB discontinuity from the AlpArray-EASI data along with velocity perturbations from P-wave tomography in the upper mantle background (Babuška *et al*., 1990) and velocity perturbation contours from tomography by Karousová *et al*. (2013). The green line approximates the European and Adriatic plate contact. Characteristic bipolar patterns of distributions of travel-time deviations are shown in the P-spheres of two stations, one with the Moldanubian pattern (fast direction dipping to the S-SW) and the second with reversed Adriatic pattern. Mantle-lithosphere domains are delimited according to their fabrics (e.g. Babuška and Plomerová, 2013).

4. Concluding remarks

We present a brief overview of the historical development of the Earth stratification, its inner discontinuities/transitions, and concentrate on definitions and modelling the LAB. In our model, we define the LAB as a transition between fossil anisotropy in the mantle-lithosphere domains and anisotropy related to the present-day flow in the asthenosphere, and suggest the global LAB model from anisotropic parameters of surface waves and the regional model of European LAB from anisotropic parameters of body waves.

The global model from (ψ_G, ξ) of surface waves shows the long wave-length features with an adequate lateral smearing, whereas the regional models from body waves are able to detect distinct LAB relief variations with short wave lengths as well as the step-like thinning/thickening of the lithosphere related to prominent sutures. Inclined fabrics within individual domains of the lithosphere and predominantly sub-horizontal orientation of the fast velocities in the asthenosphere increase the velocity contrast at the lithosphere-asthenosphere boundary and confine the LAB transition to a narrower zone than that produced by compositional or thermal variations. Taking into account differences in vertical and lateral resolution, our global and regional models are in agreement in overlapping regions.

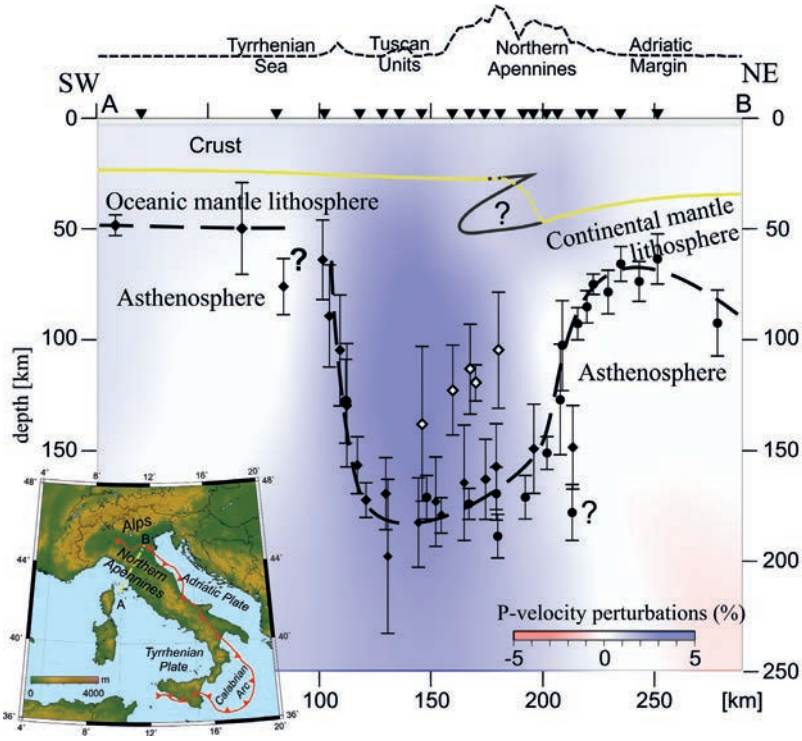

Fig. 20 - Model of shallow oceanic LAB beneath the Tyrrhenian Sea and ~200 km deep Apennines root of the ~80 km thick subducted Adriatic plate (after Munzarová *et al*., 2013) from data of the RETREAT experiment (Margheriti *et al*., 2006) with the use of modified crust (black). The crust in yellow according to Di Stefano *et al*. (2011) results in too shallow LAB (white squares). Velocity perturbations from combined P and S tomography image the steep Apenninic root extending to -300 km depth (Benoit *et al*., 2001).

Looking at the LAB with different optics and analysing different physical parameters jointly help us to understand what the LAB, MLD, and other discontinuities and transition zones both in the lithosphere and in the upper mantle mean, how the LAB is related to the lithosphere base, what is the LAB at all and how we are able to visualise it.

Acknowledgements. Cooperation with many colleagues-members of several working groups formed for individual passive seismic experiments as well as discussions with S-I. Karato are greatly appreciated. R.C. Liebermann is acknowledged for his English proof. The long-term research was step-by-step supported by national agencies - GAAV, GACR and the most recently by Operational Programme Research, Development and Education project CzechGeo/EPOS-Sci, no. CZ.02.1.01/0.0/0.0/16_013/0001800. The paper refers to the keynote "Inge Lehmann Lecture" presented at the General Assembly of the European Seismological Commission held in Valletta, Malta, from 2 to 7 September 2018.

REFERENCES

Abt D.L., Fischer K.M., French S.W., Ford A.H., Yuan H. and Romanowicz B.; 2010: *North American lithospheric discontinuity structure emaged by PS and SP receiver functions*. J. Geophys. Res., **115**, B09301, doi: 10.1029/2009JB006914.

Afonso J.C., Fernandez M., Ranalli G., Griffin W.L. and Connolly J.A.D.; 2008: *Integrated geophysical - petrological modeling of the lithosphere and sublithospheric upper mantle: methodology and applications*. Geochem. Geophys. Geosyst., **9**, Q05008, doi: 10.1029/2007GC001834.

Anderson D.L.; 1979: *Deep structure of continents*. J. Geophys. Res., **84**, 7555-7560.

Anderson D.L.; 2007: *New theory of the Earth*. Cambridge University Press, 400 pp., doi: 10.1017/CBO9781139167291.

Aric K., Gutdeutsch R., Leichter B., Lenhardt W., Plomerová J., Babuška V., Pajdušák P. and Nixdorf U.; 1989: *Structure of the lithosphere in the eastern Alps derived from P-residual analysis*. Arbeiten aus Zentralanstalt für Meteorologie und Geodynamik, Wien, Austria, Nr. 370, 26 pp.

Artemieva I.M.; 2018: *Lithosphere structure in Europe from thermal isostasy*. Earth Sci. Rev., **188**, 454-488, doi: 10.1016/j.earscirev.2018.11.004.

Artemieva I.M. and Mooney W.D.; 2001: *Thermal thickness and evolution of Precambrian lithosphere: a global study*. J. Geophys. Res. Solid Earth, **106,** 16387-16414, doi: 10.1029/2000JB900439.

Auer L., Becker T.W., Boschi L. and Schmerr N.; 2015: *Thermal structure, radial anisotropy, and dynamics of oceanic boundary layers*. Geophys. Res. Lett., **42**, 9740-9749, doi: 10.1002/2015GL066246.

Aulbach S., Massuyeau M. and Gaillard F.; 2017: *Origins of the cratonic mantle discontinuities: a view from petrology, geochemistry and thermodynamic models*. Lithos, **268,** 364-382, doi: 10.1016/j.lithos.2016.11.004.

Babuška V. and Cara M.; 1991: *Seismic anisotropy in the Earth*. Kluwer Acad. Publ., Dordrecht, The Netherlands, 217 pp.

Babuška V. and Plomerová J.; 2004: *Sorgenfrei - Tornquist zone as the mantle edge of Baltica lithosphere: new evidence from three-dimensional seismic anisotropy*. Terra Nova, **16**, 243-249.

Babuška V. and Plomerová J.; 2013: *Boundaries of mantle - lithosphere domains in the Bohemian Massif as extinct exhumation channels for high pressure rocks*. Gondwana Res., **23**, 973-987, doi: 10.1016/j.gr.2012.07.005.

Babuška V. and Plomerová J.; 2017: *Lateral displacement of crustal units relative to underlying mantle - lithosphere: example from the Bohemian Massif*. Gondwana Res., **52**, 125-138, doi: 10.1016/j.gr.2017.08.008.

Babuška V., Plomerová J. and Šílený J.; 1984: *Spatial variations of P residuals and deep structure of the European lithospere*. Geophys. J. R. Astron. Soc., **79**, 363-383.

Babuška V., Plomerová J. and Šílený J.; 1987: *Structural model of the subcrustal lithosphere in central Europe*. In: Froidevaux C. and Fuchs K. (eds), The composition, structure and dynamics of the lithosphere - asthenosphere system, AGU Geophys. Series, **16**, 239-251.

Babuška V., Plomerová J. and Granet M.; 1990: *The deep lithosphere in the Alps: a model inferred from P residuals*. Tectonophys., **176**, 137-165.

Babuška V., Montagner J.-P., Plomerová J. and Girardin N.; 1998: *Age dependent large scale fabric of the mantle - lithosphere as derived from surface wave velocity anisotropy*. Pure Appl. Geophys., **151**, 257-280.

Babuška V., Plomerová J., Vecsey L., Granet M. and Achauer U.; 2002: *Seismic anisotropy of the French Massif Central and predisposition of Cenozoic rifting and volcanism by Variscan suture hidden in the mantle - lithosphere*. Tectonics, **21**, 1-20, doi: 10.1029/2001TC901035.

Baer M.; 1980: *Relative travel time residuals for teleseismic events at the new Swiss station Network*. Ann. Geophys., **36**, 119-126.

Barruol G. and Granet M.; 2002: *A Tertiary asthenospheric flow beneath the southern French Massif Central indicated by upper mantle seismic anisotropy and related to the West Mediterranean extension*. Earth Planet. Sci. Lett., **202,** 31-48, doi: 10.1016/S0012-821X(02)00752-5.

Becker T.W., Conrad C.P., Schaeffer A.J. and Lebedev S.; 2014: *Origin of azimuthal seismic anisotropy in oceanic plates and mantle*. Earth Planet. Sci. Lett., **401**, 236-250.

Beghein C., Yuan K., Schmerr N. and Xing Z.; 2014: *Changes in seismic anisotropy shed light on nature of the Gutenberg discontinuity*. Sci., **343**, 1237-1240.

Ben Ismail W. and Mainprice D.; 1998: *An olivine fabric database: an overview of upper mantle fabrics and seismic anisotropy*. Tectonophys., **296**, 145-157, doi: 10.1016/S0040-1951(98)00141-3.

Benoit M.H., Torpey V., Liszewski K., Levin V. and Park J.; 2011: *P and S wave upper mantle seismic velocity structure beneath the northern Apennines: new evidence for the end of subduction*. Geochem. Geophys. Geosyst., **12**, Q06004, doi: 10.1029/2010GC003428.

Bodin T., Leiva J., Romanowicz B., Maupin V. and Yuan H.; 2016: *Imaging anisotropic layering with Bayesian inversion of multiple data types*. Geophys. J. Int., **206**, 605-629, doi: 10.1093/gji/ggw124.

Bruneton M., Pedersen H.A., Kukkonen I.T., Arndt N.T., Funke S., Friedrich W., Farra V., Vacher P. and SVEKALAPKO Seismic Tomography Working Group; 2004: *Layered lithospheric - mantle in the central Baltic Shield from surface waves and xenolith analysis*. Earth Planet. Sci. Lett., **226**, 41-52, doi: 10.1016/j.epsl.2004.07.034.

Burgos G., Montagner J.-P., Beucler E., Capdeville Y., Mocquet A. and Drilleau B.; 2014: *Oceanic lithospher - asthenosphere boundary from surface wave dispersion data*. J. Geophys. Res. Solid Earth, **119**, 1079-1093.

Calò M., Bodin T. and Romanowicz B.; 2016: *Layered structure in the upper mantle across northern American from joint inversion of long and short period seismic data*. Earth Planet. Sci. Lett., **449**, 164-175.

Chen T., Liebermann R.C., Zou Y., Li Y., Qi X. and Li B.; 2017: *Tracking silica in Earth's upper mantle using new sound velocity data for coesite to 5.8 GPa and 1073 K*. Geophys. Res. Lett., **44**, 7757-7765, doi: 10.1002/2017GL073950.

Chyba J., Plomerová J., Vecsey L. and Munzarová H.; 2017: *Tomography study of the upper mantle around the TESZ based on PASSEQ experiment data*. Phys. Earth Planet. Inter., **266**, 29-38, doi: 10.1016/j.pepi.2017.01.002.

Cooper C.M., Miller M.S. and Moresi L.; 2017: *The structural evolution of the deep continental lithosphere*. Tectonophys., **695**, 100-121.

Cotte N., Pedersen H.A. and TOR Working Group; 2002: *Sharp contrast in lithospheric structure across the Sorgenfrei - Tornquist Zone as inferred by Rayleigh wave analysis of TOR1 project data*. Tectonophys., **360**, 75-88.

Dando B.D.E., Stuart G.W., Houseman G.A., Hegedus E., Bruckl E. and Radovanovic S.; 2011: *Teleseismic tomography of the mantle in the Carpathian - Pannonian Region of central Europe*. Geophys. J. Int., **186**, 11-31, doi: 10.1111/j.1365-246X.2011.04998.x.

Darbyshire F.A., Eaton D.W., Frederiksen A.W. and Ertolahti L.; 2007: *New insights into the lithosphere beneath the Superior Province from Rayleigh wave dispersion and receiver function analysis*. Geophys. J. Int., **169**, 1043-1068, doi: 10.1111/j.1365-246X.2006.03259.x.

Debayle E. and Kennett B.L.N.; 2000: *The Australian upper mantle: structure and deformation inferred from surface waves*. J. Geophys. Res., **105**, 25423-25450.

Debayle E. and Richard Y.; 2013: *Seismic observations of large scale deformation at the bottom of fast moving plates*. Earth Planet. Sci. Lett., **376**, 165-177.

Di Stefano R., Bianchi I., Ciaccio M.G., Carrara G. and Kissling E.; 2011: *Three dimensional Moho topography in Italy: new constraints from receiver functions and controlled source seismology*. Geochem. Geophys. Geosyst., **12**, Q09006, doi: 10.1029/2011GC003649.

Dziewonski A.M. and Anderson D.L.; 1981: *Preliminary reference Earth model*. Phys. Earth Planet. Inter., **25**, 297-356.

Eaton D.W., Darbyshire F., Evans R.L., Grütter H., Jones A.G. and Yuan X.; 2009: *The elusive lithosphere - asthenosphere boundary (LAB) beneath cratons*. Lithos, **109**, 1-22.

Eken T., Plomerová J., Vecsey L., Babuška V., Roberts R., Shomali H. and Bodvarson R.; 2012: *Effects of seismic anisotropy on P-velocity tomography of the Baltic Shield*. Geophys. J. Int., **188**, 600-612, doi: 10.1111/j.1365-246X.2011.05280.x.

Ferreira A., Woodhouse J., Visser K. and Trampert J.; 2010: *On the robustness of global radial anisotropic surface wave tomography*. J. Geophys. Res. Solid Earth, **115**, B04313, doi: 10.1029/2009JB006716.

Fischer K.M., Ford H.A., Abt D.L. and Rychert C.A.; 2010: *The lithosphere - asthenosphere boundary*. Ann. Rev. Earth Planet. Sci., **38**, 551-575, doi: 10.1146/annurev-earth-040809-152438.

Frederiksen A.W., Bostock M.G. and Cassidy J.F.; 2001: *S-wave velocity structure of the Canadian upper mantle*. Phys. Earth Planet. Inter., **124**, 175–191.

Fullea J., Afonso J.C., Connolly J.A.D., Fernàndez M., García-Castellanos D. and Zeyen H.; 2009: *LitMod3D: an interactive 3-D software to model the thermal, compositional, density, seismological, and rheological structure of the lithosphere and sublithospheric upper mantle*. Geochem. Geophys. Geosyst., **10**, Q08019, doi: 10.1029/2009GC002391.

Funke S., Friedrich W. and SVEKALAPKO Seismic Tomography Working Group; 2003: *Evidence for a continental keel beneath the Palaeoproterozoic Svecifennian Orogen in Fennoscandia from surface wave tomography*. In: Abstract, EGU-AGU Joint Meeting, Nice, France, EAE03-A-02712.

Gaherty J.B. and Jordan T.H.; 1995: *Lehmann discontinuity as the base of an anisotropic layer beneath continents*. Sci., **268**, 1468-1471.

Geissler W.H., Sodoudi F. and Kind R.; 2010: *Thickness of the central and eastern European lithosphere as seen by S receiver functions*. Geophys. J. Int., **181**, 604-634.

Gradmann S., Ebbing J. and Fullea J.; 2013: *Integrated geophysical modelling of a lateral transition zone in the lithospheric mantle under Norway and Sweden*. Geophys. J. Int., **194**, 1358-1373, doi: 10.1093/gji/ggt213.

Grand S.P. and Helmberger D.V.; 1984: *Upper mantle shear structure beneath the northwest Atlantic Ocean*. Geophys. J. R. Astron. Soc., **76**, 399-438.

Granet M., Wilson M. and Achauer U.; 1995: *Imaging a mantle plume beneath the Massif Central (France)*. Earth Planet. Sci. Lett., **17**, 1109-1112.

Gregersen S., Voss P. and TOR Working Group; 2002: *Summary of project TOR: delineation of stepwise, sharp, deep lithosphere transition across Germany - Denmark - Sweden*. Tectonophys., **360**, 61-73.

Gung Y., Panning M. and Romanowicz B.; 2003: *Global anisotropy and the thickness of continents*. Nat., **422**, 707-711.

Gutenberg B.; 1959: *Physics of the Earth's interior, 1st ed*. Elsevier, Amsterdam, The Netherlands, 252 pp.

Hales A.L.; 1969*: A seismic discontinuity in the lithosphere*. Earth Planet. Sci. Lett., **7**, 44-46, doi: 10.1016/0012-821X(69)90009-0.

Halley E.; 1692: *An account of the cause of the change of the variation of the magnetical needle; with an hypothesis of the structure of the internal parts of the Earth, as it was proposed to the Royal Society in one of their late meetings*. Philosophical Transactions (1683-1775), **16**, 563-578.

Hess H.; 1964: *Seismic anisotropy of the upper mantle under oceans*. Nat., **203**, 629-631.

Hetényi G., Molinari I., Clinton J., Bokelmann G., Bondár I., Crawford W.C., Dessa J.-X., Doubre C., Friederich W., Fuchs F., Giardini D., Gráczer Z., Handy M.R., Herak M., Jia Y., Kissling E., Kopp H., Korn M., Margheriti L., Meier T., Mucciarelli M., Paul A., Pesaresi D., Piromallo C., Plenefisch T., Plomerová J., Ritter J., Rümpker G., Šipka V., Spallarossa D., Thomas C., Tilmann F., Wassermann J., Weber M., Wéber Z., Wesztergom V., Živčić M., AlpArray Seismic Network Team, AlpArray OBS Cruise Crew and AlpArray Working Group; 2018a: *The AlpArray Seismic Network - a large-scale European experiment to image the Alpine orogeny*. Surv. Geophys., **39**, 1009-1033, doi: 10.1007/s10712-018-9472-4.

Hetényi G., Plomerová J., Bianchi I., Kampfová Exnerová H., Bokelmann G., Handy M.R., Babuška V. and AlpArray-EASI Working Group; 2018b: *From mountain summits to roots: crustal structure of the eastern Alps and Bohemian Massif along longitude 13.3°E*. Tectonophys., **744**, 239-255, doi: 10.1016/j.tecto.2018.07.001.

Hjelt S.-E., Korja T., Kozlovskaya E., Lahti I., Yliniemi J., BEAR and SVEKALAPKO Seismic Tomography Working Groups; 2006: *Electrical conductivity and seismic velocity structures of the lithosphere beneath the Fennoscandian Shield*. Geological Society, London, Memoirs, **32**, 541-559, doi: 10.1144/GSL.MEM.2006.032.01.33.

Hopper E. and Fischer K.M.; 2015: *The meaning of mid-lithsopheri discontinuities: a case study in the northern U.S. Craton*. Geochem. Geophys. Geosyst., **16**, 4057-4083.

Jackson I. and Faul U.H.; 2010: *Grainsize sensitive viscoelastic relaxation in olivine: towards a robust laboratory based model for seismological application*. Phys. Earth Planet. Inter., **183**, 151-163, doi: 10.1016/j.pepi.2010.09.005.

Jones A.G., Plomerová J., Korja T., Sodoudi F. and Spakman W.; 2010: *Europe from the bottom up: a statistical examination of the central and northern European lithosphere - asthenosphere boundary from comparing seismological and electromagnetic observations*. Lithos, **120**, 14-29, doi: 10.1016/j.lithos.2010.07.013.

Judenherc S., Granet M., Brun J.-P., Poupinet G., Plomerová J., Mocquet A. and Achauer U.; 2002: *Images of lithospheric heterogeneities in the Armorican segment of the Hercynian range in France*. Tectonophys., **358**, 121-134.

Karato S.-I. and Park J.: 2019: *On the origin of the upper mantle discontinuities*. In: Yuan H. and Romanowicz B. (eds), Lithospheric discontinuities, American Geophysical Union, Geophysical Monograph Series, **239**, 5-34.

Karato S., Olugboji T.M. and Park J.; 2015: *Mechanisms and geologic significance of the mid-lithosphere discontinuity in the continents*. Nat. Geosci., **8**, 509-514.

Karousová H., Plomerová J. and Babuška V.; 2013: *Upper mantle structure beneath the southern Bohemian Massif and its surroundings imaged by high resolution tomography*. Geophys. J. Int., **194**, 1203-1215, doi: 10.1093/gji/ggt159.

Kind R. and Yuan X.; 2019*: Perspectives of the S-receiver function method to image upper mantle discontinuities*. In: Yuan H. and Romanowicz B. (eds), Lithospheric discontinuities, American Geophysical Union, Geophysical Monograph Series, **239**, 139-154.

Kind R., Handy M.R., Yuan H.X., Meier T., Kämpf H. and Soomro R.; 2017: *Detection of a new sub-lithospheric discontinuity in central Europe with S-receiver functions*. Tectonophys., **700**, 19-31, doi: 10.1016/j.tecto.2017.02.002.

Korja T.; 2007: *How is the European lithosphere imaged by magnetotellurics?* Surv. Geophys., **28**, 239-272.

Lehmann I.; 1936: *P'*. Bureau Central Sismologique International, Ser. A, Travaux Scientifique, **14**, 87-115.

Lehmann I.; 1959: *The interior of the Earth as revealed by earthquakes*. Ann. Geophys., **15**, 93-118.

Lehmann I.; 1961: *S and the structure of the upper mantle*. Geophys. J. R. Astr. Soc., **4**, 124-138.

Li A. and Burke K.; 2006: *Upper mantle structure of southern Africa from Rayleigh wave tomography*. J. Geophys. Res., **111**, B10303, doi: 10.1029/2006JB004321.

Lippitsch R., Kissling E. and Ansorge J.; 2003: *Upper mantle structure beneath the Alpine Orogen from high resolution teleseismic tomography*. J. Geophys. Res., **108,** B82376, doi: 10.1029/2002JB002016.

Margheriti L., Pondrelli S., Piccinini D., Piana Agostinetti N., Lucente F.P., Amato A., Baccheschi P., Giovani L., Salimbeni S., Park J., Brandon M., Levin V., Plomerová J., Jedlička P., Vecsey L., Babuška V., Fiaschi A., Carpani B. and Ulbricht P.; 2006: *The subduction structure of the northern Apennines: results from the RETREAT seismic deployment*. Ann. Geophys., **49**, 1119-1131.

Medhus A.B., Balling N., Jacobsen B.H., Weidle C., England R.W., Kind R., Thybo H. and Voss P.; 2012: *Upper mantle structure beneath the southern Scandes Mountains and the northern Tornquist Zone revealed by P-wave travel time tomography*. Geophys. J. Int., **189**, 1315-1334, doi: 10.1111/j.1365-246X.2012.05449.x.

Mitterbauer U., Behm M., Brueckl E., Lippitsch R., Guterch A., Keller G.R., Kozlovskaya E., Rumpfhuber E.M. and Sumanovic F.; 2011: *Shape and origin of the East Alpine Slab constrained by the ALPASS teleseismic model*. Tectonophys., **510,** 195-206.

Montagner J.-P. and Anderson D.L.; 1989: *Constrained reference mantle model*. Phys. Earth Planet. Inter., **58**, 205-227.

Montagner J.-P. and Tanimoto T.; 1991: *Global upper mantle tomography of seismic velocities and anisotropies*. J. Geophys. Res., **96**, 20337-20351.

Montagner J.-P. and Burgos G.; 2019: *Lithospheric and Asthenospheric Structure below oceans from anisotropic tomography*. In: Yuan H. and Romanowicz B. (eds), Lithospheric discontinuities, American Geophysical Union, Geophysical Monograph Series, **239**, 55-69.

Mueller S.; 1982*: Deep structure and recent dynamics in the Alps*. In: Hsü K. (ed), Mountain building processes, Acad. Press, London, U.K., pp. 85-93.

Munzarová H., Plomerová J., Babuška V. and Vecsey L.; 2013: *Upper mantle fabrics beneath the northern Apennines revealed by seismic anisotropy*. Geochem. Geophys. Geosyst., **14**, 1156-1181, doi: 10.1002/ggge.20092.

Munzarová H., Plomerová J. and Kissling E.; 2018a: *Novel anisotropic teleseismic body-wave tomography code AniTomo to illuminate heterogeneous anisotropic upper mantle: part I - theory and inversion tuning with realistic synthetic data*. Geophys. J. Int., **215,** 524-545, doi: 10.1093/gji/ggy296.

Munzarová H., Plomerová J., Kissling E., Vecsey L. and Babuška V.; 2018b: *Novel anisotropic teleseismic body-wave tomography code AniTomo to illuminate heterogeneous anisotropic upper mantle: part II - application to data of passive seismic experiment LAPNET in northern Fennoscandia*. Geophys. J. Int., **215**, 1388-1409, doi: 10.1093/gji/ggy327.

Olugboji T.M., Karato S-I. and Park J.; 2013: *Structures of the oceanic lithosphere - asthenosphere boundary: mineralphysics modeling and seismological signatures*. Geochem. Geophys. Geosyst., **14**, 880-901, doi: 10.1002/ggge.20086.

Pedersen H.A., Debayle E., Maupin V. and POLENT/LAPNET Working Group; 2013: *Strong lateral variations of lithospheric mantle beneath cratons - example from the Baltic Shield*. Earth Planet. Sci. Lett., **383**, 164-172.

Peltonen P. and Brügmann G.; 2006: *How old is the continental mantle of the Karelian Craton?* In: Abstracts, Peltonen P. and Pasanen A. (eds), 27th Nordic Geological Winter Meeting, Oulu, Finland, Bull. Geol. Soc. Finland, Special Issue I, p. 122.

Plomerová J. and Babuška V.; 2010: *Long memory of mantle lithosphere fabric - European LAB constrained from seismic anisotropy*. Lithos, **120**, 131-143.

Plomerová J., Babuška V., Šílený J. and Horálek J.; 1998: *Seismic anisotropy and velocity variations in the mantle beneath the Saxothuringicum - Moldanubicum contact in central Europe*. Pure Appl. Geophys., **151**, 365-394.

Plomerová J., Babuška V., Vecsey L., Kouba D. and TOR Working Group; 2002a: *Seismic anisotropy of the lithosphere around the Trans-European Suture Zone (TESZ) based on teleseismic body-wave data of the TOR experiment*. Tectonophys., **360**, 89-114.

Plomerová J., Kouba D. and Babuška V.; 2002b: *Mapping the lithosphere - asthenosphere boundary (LAB) through changes in surface wave anisotropy*. Tectonophys., **358**, 175-185.

Plomerová J., Margheriti L., Park J., Babuška V., Pondrelli S., Vecsey L., Piccinini D., Levin V., Baccheschi P. and Salimbeni S.; 2006: *Seismic anisotropy beneath the northern Apennines (Italy): mantle flow or lithosphere fabric?* Earth Planet. Sci. Lett., **247**, 157-170.

Plomerová J., Achauer U., Babuška V., Vecsey L. and BOHEMA Working Group; 2007: *Upper mantle beneath the Eger Rift (central Europe): plume or asthenosphere upwelling?* Geophys. J. Int., **169,** 675-682; doi: 10.1111/j.1365-246X.2007.03361.x.

Plomerová J., Babuška V., Kozlovskaya E., Vecsey L. and Hyvonen L.T.; 2008: *Seismic anisotropy - a key to resolve fabrics of mantle lithosphere of Fennoscandia*. Tectonophys., **462**, 125-136, doi: 10.1016/j.tecto.2008.03.018.

Plomerová J., Munzarová H., Vecsey L., Kissling E., Achauer U. and Babuška V.; 2016: *Cenozoic volcanism in the Bohemian Massif in the context of P- and S-velocity high-resolution teleseismic tomography of the upper mantle*. Geochem., Geophys., Geosyst., **17**, 1–24, doi: 10.1002/2016GC006318.

Praus O., Pěčová J., Petr V., Babuška V. and Plomerová J.; 1990: *Magnetotelluric and seismological determination of the lithosphere - asthenosphere transition in central Europe*. Phys. Earth Planet. Inter., **60**, 212-228.

Priestley K. and Debayle E.; 2003: *Seismic evidence for a moderately thick lithosphere beneath the Siberian Platform*. Geophys. Res. Lett., **30**, 1118, doi: 10.1029/2002GL015931.

Priestley K. and McKenzie; 2013: *The relation between shear wave velocity, temperature, attenuation and viscosity in the shallow part of the mantle*. Earth Planet. Sci. Lett., **381**, 78-79.

Priestley K., McKenzie D. and Ho T.; 2019: *A lithosphere - asthenosphere boundary - a global model derived from multimode surface wave tomography and petrology*. In: Yuan H. and Romanowicz B. (eds), Lithospheric discontinuities, American Geophysical Union, Geophysical Monograph Series, **239**, 111-123.

Revenaugh J. and Jordan T.H.; 1991: *Mantle layering from ScS reverberation*. J. Geophys. Res., **96**, 19781-19810, doi: 10.1029/91JB01487.

Ritter J.R.R., Jordan M., Christensen U.R. and Achauer U.; 2001: *A mantle plume below the Eifel volcanic fields, Germany*. Earth Planet. Sci. Lett., **186**, 7-14.

Rychert C.A. and Schearer P.M.; 2009: *A global view of the lithosphere - asthenosphere boundary*. Sci., **324**, 495-498.

Rychert C.A., Harmon N. and Tharimena S.; 2019: *Seismic imaging of the base of the oceanic plates*. In: Yuan H. and Romanowicz B. (eds), Lithospheric discontinuities, American Geophysical Union, Geophysical Monograph Series, **239**, 71-87.

Sandoval S., Kissling E., Ansorge J. and SVEKALAPKO Seismic Tomography Work; 2004: *High resolution body wave tomography beneath the SVEKALAPKO array - II. Anomalous upper mantle structure beneath the central Baltic Shield*. Geophys. J. Int., **157**, 200-214.

Savage M.K. and Siver P.G.; 2008: *Evidence for a compositional boundary within the lithospheric mantle beneath the Kalahari Craton from S receiver functions*. Earth. Planet. Sci. Lett., **272**, 600-609.

Schmerr N.; 2012: *The Gutenberg discontinuity: melt at the lithosphere - asthensophere boundary*. Sci., **335**, 1480-1483, doi: 10.1126/science.1215433.

Schulmann K.; 2009: *Mechanics of Variscan Orogeny: a modern view on orogenic research*. C. R. Geosci., **341,** 97-102, doi: 10.1016/j.crte.2009.01.003.

Selway K.; 2019: *Electrical discontinuities in the continental lithosphere imaged with Magnetotellurics*. In: Yuan H. and Romanowicz B. (eds), Lithospheric discontinuities, American Geophysical Union, Geophysical Monograph Series, **239**, 89-109.

Shearer P.M.; 1990: *Seismic imaging of upper-mantle structure with new evidence for a 520 km discontinuity*. Nat., **344**, 121-126.

Silvennoinen H., Kozlovskaya E., Kissling E., Kosarev G. and POLENET/LAPNET Working Group; 2014: *A new Moho boundary map for northern Fennoscandian Shield based on combined controlled source seismic and receiver function data*. Geophys. Res. J., **1-2,** 19-32, doi: 10.1016/j.grj.2014.03.001.

Silvennoinen H., Kozlovskaya E. and Kissling E.; 2016: *POLENET/LAPNET teleseismic P wave travel time tomography model of the upper mantle beneath northern Fennoscandia*. Solid Earth, **7**, 425-439, doi: 10.5194/se-7-425-2016.

Simons F.J. and van der Hilst R.D.; 2002: *Age-dependent seismic thickness and mechanical strength of the Australian lithosphere*. Geophys. Res. Lett., **29**, 1529, doi: 10.1029/2002GL014962.

Sobolev S.V., Zeyen H., Granet M., Achauer U., Bauer C., Werling F., Altherr R. and Fuchs K.; 1997: *Upper mantle temperatures and lithosphere-asthenosphere system beneath the French Massif Central constrained by seismic, gravity, petrological and thermal observations*. Tectonophys., **275**, 143–164.

Song X. and Helmberger D.V.; 1998: *Seismic evidence for an inner core transition zone*. Sci., **282**, 924-927, doi: 10.1126/science.282.5390.924.

TRANSALP Working Group; 2001: *European orogenic processes research transects the eastern Alps*. Eos Trans. AGU, **82**, 453, 460-461.

Vecsey L., Plomerová J., Kozlovskaya E. and Babuška V.; 2007: *Shear-wave splitting as a diagnostic of varying upper mantle structure beneath south-eastern Fennoscandia*. Tectonophys., **438**, 57–77, doi: 10.1016/j.tecto.2007.02.017.

Vecsey L., Plomerová J., Babuška V. and PASSEQ Working Group; 2014: *Mantle lithosphere transition from the East European Craton to the Variscan Bohemian Massif imaged by shear-wave splitting*. Solid Earth, **5**, 779-792, doi: 10.5194/se-5-779-2014.

Walker K.T., Bokelmann G.H.R., Klemperer S.L. and Bock G.; 2004: *Shear-wave splitting around the Eifel Hotspot: evidence for a mantle upwelling*. Geophys. J. Int., **163**, 962-980, doi: 10.1111/j.1365-246X.2005.02636.x.

Weeraratne D.S., Forsyth D.W., Fischer K.M. and Nyblade A.A.; 2003: *Evidence for an upper mantle plume beneath the Tanzanian Craton from Rayleigh wave tomography*. J. Geophys. Res., **108**, 2427, doi: 10.1029/2002JB002273.

Wegener A.L.; 1915: *The origin of continents and oceans*. Druck und Verlag von Friedr. Vieweg & Sohn, Braunschweig, Germany, 94 pp.

Wilde-Piórko M., Geissler W.H., Plomerová J., Grad M., Babuška V., Brückl E., Cyziene J., Czuba W., England R., Gaczyński E., Gazdova R., Gregersen S., Guterch A., Hanka W., Hegedűs E., Heuer B., Jedlička P., Lazauskiene J., Keller G.R., Kind R., Klinge K., Kolínský P., Komminaho K., Kozlovskaya E., Krüger F., Larsen T., Majdański M., Málek J., Motuza G., Novotný O., Pietrasiak R., Plenefisch T., Růžek B., Sliaupa S., Środa P., Świeczak M., Tiira T., Voss P. and Wiejacz P.; 2008: *PASSEQ 2006-2008: passive seismic experiment in Trans-European Suture Zone*. Stud. Geophys. Geod., **52**, 439-448, doi: 10.1007/s11200-008-0030-2.

Yuan H. and Romanowicz B.; 2019: *Introduction - Lithospheric discontinuities*. American Geophysical Union, Geophysical Monograph Series, **239**, 1-3.

Corresponding author: Jaroslava Plomerová
Institute of Geophysics, Czech Academy of Sciences
Boční II, 14131 Prague 4, Czech Republic
Phone: +420 267 103391; e-mail: jpl@ig.cas.cz